NAVAL POSTGRADUATE SCHOOL
Monterey, California

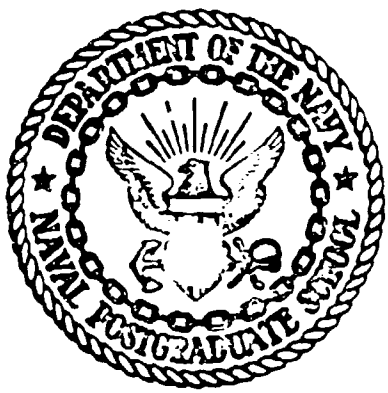

THESIS

SIMULTANEOUS IDENTIFICATION OF SHORT PERIOD AND PHUGOID PARAMETERS USING AN ADVANCED LIKELIHOOD METHOD

BY

Frederick T. Bryan

December 1975

Thesis Advisor Ronald A. Hess

Approved for public release; distribution unlimited.

UNCLASSIFIED

SECURITY CLASSIFICATION OF THIS PAGE (When Data Entered)

REPORT DOCUMENTATION PAGE	READ INSTRUCTIONS BEFORE COMPLETING FORM
1. REPORT NUMBER	2. GOVT ACCESSION NO. 3. RECIPIENT'S CATALOG NUMBER
4. TITLE (and Subtitle) (6) SIMULTANEOUS IDENTIFICATION OF SHORT PERIOD AND PHUGOID STABILITY PARAMETERS USING AN ADVANCED LIKELIHOOD METHOD.	5. TYPE OF REPORT & PERIOD COVERED Aeronautical Engineer December 1975
	6. PERFORMING ORG. REPORT NUMBER
7. AUTHOR(s) (10) Frederick T. Bryan, Major, USMC	8. CONTRACT OR GRANT NUMBER(s) (9) Master's thesis,
9. PERFORMING ORGANIZATION NAME AND ADDRESS Naval Postgraduate School Monterey, California 93940	10. PROGRAM ELEMENT, PROJECT, TASK AREA & WORK UNIT NUMBERS (12) 119p.
11. CONTROLLING OFFICE NAME AND ADDRESS (11) Naval Postgraduate School Monterey, California 93940	12. REPORT DATE Dec[illegible]975 13. NUMBER OF PAGES 120
14. MONITORING AGENCY NAME & ADDRESS(if different from Controlling Office) Naval Postgraduate School Monterey, California 93940	15. SECURITY CLASS. (of this report) Unclassified 15a. DECLASSIFICATION/DOWNGRADING SCHEDULE

16. DISTRIBUTION STATEMENT (of this Report)

Approved for public release; distribution unlimited

17. DISTRIBUTION STATEMENT (of the abstract entered in Block 20, if different from Report)

18. SUPPLEMENTARY NOTES

19. KEY WORDS (Continue on reverse side if necessary and identify by block number)

Maximum Likelihood Identification
Stability Parameters
Stability Derivatives
Flight Test Data Reduction

20. ABSTRACT (Continue on reverse side if necessary and identify by block number)

An investigation was conducted to determine the feasibility of obtaining the short period and phugoid stability derivatives from one maneuver, "simultaneously". It was concluded that the maximum likelihood identification program SCIDNT I showed great promise in obtaining the short period and phugoid stability derivatives from one maneuver. Extraction of the short period stability parameters in the presence of the phugoid was easy, straight forward, and yielded results similar to those obtained from pure short period → to next in 1473B

DD FORM 1 JAN 73 1473 A EDITION OF 1 NOV 65 IS OBSOLETE (Page 1) S/N 0102-014-6601

UNCLASSIFIED

SECURITY CLASSIFICATION OF THIS PAGE (When Data Entered)

251450

from previous page 1473A

data. Estimation of the phugoid stability parameters (Theta) was possible when they were estimated in conjunction with Z_{δ_o}, X_{δ_o}, M_{δ_o}, and θ_{δ_o}. It was recommended that a new set of data be obtained at a flight condition where the phugoid is at least moderately damped and that this data be analyzed to resolve the present anomalies.

1473B

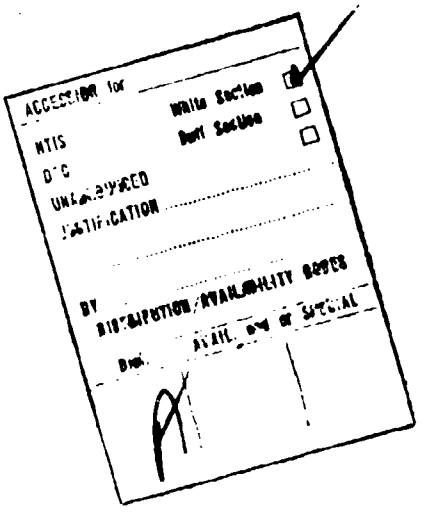

SIMULTANEOUS IDENTIFICATION OF SHORT PERIOD AND PHUGOID STABILITY PARAMETERS USING AN ADVANCED MAXIMUM LIKELIHOOD METHOD

by

Frederick T. Bryan
Major United States Marine Corps
B.S.B.A., Boston College 1963
M.S.A.E., Naval Postgraduate School, 1974

Submitted in partial fulfillment of the
requirements for the degree of

AERONAUTICAL ENGINEER

from the

NAVAL POSTGRADUATE SCHOOL

December 1975

Author: Frederick T. Bryan

Approved by: Ronald A. Hess
Thesis Advisor

L. V. Schmidt
Second Reader

Richard W. Bell
Chairman, Department of Aeronautics

Academic Dean

ABSTRACT

An investigation was conducted to determine the feasibility of obtaining the short period and phugoid stability derivatives from one maneuver, "simultaneously". It was concluded that the maximum likelihood identification program SCIDNT I showed great promise in obtaining the short period and phugoid stability derivatives from one maneuver. Extraction of the short period stability parameters in the presence of the phugoid was easy, straight forward, and yielded results similar to those obtained from pure short period data. Estimation of the phugoid stability parameters was possible when they were estimated in conjunction with Z_o, X_o, M_o, and θ_o. It was recommended that a new set of data be obtained at a flight condition where the phugoid is at least moderately damped and that this data be analyzed to resolve the present anomalies.

TABLE OF CONTENTS

I. INTRODUCTION..... 15
A. BACKGROUND..... 15
B. PURPOSE..... 16
C. DESCRIPTION OF AIRPLANE..... 16
D. MAXIMUM LIKELIHOOD PARAMETER IDENTIFICATION THEORY..... 16
E. MAXIMUM LIKLIHOOD IDENTIFICATION OF PARAMETERS. 19
1. Prediction Equations..... 24
2. Measurement Update Equations..... 25
3. Optimization Procedure..... 26
4. Linear Systems..... 33
5. Time Invariant Linear Systems In Statistical Steady State..... 35
6. Maximum Likelihood With No Process Or Measurement Noise..... 40
F. AIRCRAFT PARAMETER IDENTIFICATION USING THE MAXIMUM LIKELIHOOD METHOD..... 43
G. SCOPE OF RESEARCH..... 44
H. METHOD OF TESTS..... 44
II. RESULTS AND DISCUSSION..... 46
A. SHORT PERIOD AIRFRAME PARAMETER IDENTIFICATION. 46
1. Airplane Test Conditions..... 46
2. Method Of Investigation..... 46
3. Data Analysis 50
B. PHUGOID AIRFRAME PARAMETER IDENTIFICATION..... 54
1. Airplane Test Conditions..... 54
2. Method Of Investigation..... 55
3. Data Analysis..... 59
C. SIMULTANEOUS SHORT PERIOD AND PHUGOID PARAMETER IDENTIFICATION..... 62

1. Airplane Test Conditions..... 62
2. Method Of Investigation..... 63
3. Data Analysis..... 66
III. CONCLUSIONS..... 72
A. GENERAL..... 72
B. SPECIFIC..... 72
IV. RECOMMENDATIONS..... 73
APPENDIX A - TEST AIRCRAFT DESCRIPTION..... 74
APPENDIX B - DERIVATION OF THE AIRPLANE MODEL AND MEASUREMENT EQUATIONS..... 79
APPENDIX C - AIRPLANE AND GROUND DATA SYSTEMS..... 86
APPENDIX D - TIME HISTORY PITS..... 91
LIST OF REFERENCES..... 118
INITIAL DISTRIBUTION LIST..... 119

LIST OF FIGURES

1. MAXIMUM LIKELIHOOD ESTIMATES..... 18
2. LIKELIHOOD FUNCTION CHANGE DURING ITERATION FOR DOUBLET INPUT..... 48
3. LIKELIHOOD FUNCTION CHANGE DURING ITERATION FOR SINUSOIDAL INPUT..... 49
4. LIKELIHOOD FUNCTION DURING ITERATION USING 2 sps.... 57
5. LIKELIHOOD FUNCTION DURING ITERATION USING 5 sps.... 58
6. LIKELIHOOD FUNCTION DURING ITERATION FOR PHUGOID.... 64
7. LIKELIHOOD FUNCTION DURING ITERATION FOR PHUGOID (STABILITY DERIVATIVES, Z_o, X_o, M_o, AND θ_o) 66

APPENDIX A

1. F-14A AIRPLANE PHOTOGRAPHS..... 76
2. F-14A AIRPLANE PHOTOGRAPHS..... 77
3. F-14A AIRPLANE - THREE VIEW DRAWING..... 78

APPENDIX B

1. ANGLE OF ATTACK DUE TO VERTICAL VELOCITY PERTURBATION..... 82

APPENDIX D

1. SHORT PERIOD TIME HISTORY USING DOUBLET INPUT..... 91
2. SHORT PERIOD TIME HISTORY USING SINUSOIDAL INPUT.... 94
3. SHORT PERIOD TIME HISTORY WITH NON-ZERO INITIAL CONDITIONS..... 97
4. PHUGOID TIME HISTORY USING 2 SPS DATA..... 100

5. PHUGOID TIME HISTORY USING 5 SPS DATA..... 103
6. SHORT PERIOD TIME HISTORY SUPERIMPOSED ON PHUGOID... 106
7. PHUGOID TIME HISTORY WITH POSITIVE X_u 109
8. PHUGOID TIME HISTORY WITH NEGATIVE X_u 112
9. PHUGOID TIME HISTORY WITH SEVEN PARAMETERS ESTIMATED..... 115

LIST OF TABLES

I.	SHORT PERIOD TEST CONDITIONS.....	46
II.	COMPARISON OF LEAST SQUARES PARAMETER VALUES AND SCIDNT PARAMETER VALUES.....	47
III.	SCIDNT ESTIMATES OF LONGITUDINAL SHORT PERIOD STABILITY DERIVATIVES USING A DOUBLET INPUT.....	51
IV.	SCIDNT ESTIMATES OF LONGITUDINAL SHORT PERIOD STABILITY DERIVATIVES USING A SINUSOIDAL INPUT...	52
V.	COMPARISON OF LONGITUDINAL SHORT PERIOD CHARACTERISTICS.....	54
VI.	PHUGOID TEST CONDITIONS.....	54
VII.	SCIDNT ESTIMATES OF LONGITUDINAL PHUGOID STABILITY DERIVATIVES USING 2 SPS DATA.....	60
VIII.	SCIDNT ESTIMATES OF LONGITUDINAL PHUGOID STABILITY DERIVATIVES USING 5 SPS DATA.....	61
IX.	SHORT PERIOD AND PHUGOID TEST CONDITIONS.....	63
X.	SCIDNT ESTIMATES OF LONGITUDINAL SHORT PERIOD STABILITY DERIVATIVES.....	67
XI.	SCIDNT ESTIMATES OF PHUGOID STABILITY DERIVATIVES (POSITIVE X_u).....	68
XII.	SCIDNT ESTIMATES OF PHUGOID STABILITY DERIVATIVES (NEGATIVE X_u).....	69
XIII.	SCIDNT ESTIMATES OF PHUGOID STABILITY DERIVATIVES (PARAMETERS ESTIMATED WITH Z_o, X_o, M_o, and θ_o)•••	70

LIST OF SYMBOLS

LIKELIHOOD FUNCTION THEORY

B(i)	innovations covariance at point (i)
D	u coefficient matrix, measurement equation
F	linearized f matrix
G	u coefficient matrix, state equation
H	linearized h matrix
I	identity matrix
K	kalman gain
M	information matrix
P	state covariance matrix
Q	correlation matrix of w
R	correlation matrix of w
T	final time
W	equasion error method weight
X	state vector
Y	discrete measurement state vector
e	2.1718
m	number of discrete measurements
t	time
u	deterministic input vector
v	random measurement noise vector
w	random process noise vector
z	measured outcome of an actual experiment
cov	covariance
E{ }	expected value of { }
exp	exponential function of
f( )	nonlinear function of ( )
h( )	nonlinear measurement function of ( )
$\mathcal{L}$( )	likelihood function of ( )
max	maximum

$p(\ )$	probability of ( )
$Tr(\ )$	trace of matrix ( )
$(\Theta \mid z)$	function of Θ given that event z has occured
$(\ )^T$	transpose of matrix ( )
$\mid\ \mid$	absolute value
$\_(j \mid k)$	the estimate of _ at time j given measurements at times up to and including time k
$d(\ )/dt$	derivative of ( ) with respect
$(\dot{\ })$	to time, t
$(\ddot{\ })$	second derivative of ( ) with respect to time, t
$\partial(\ )/\partial[\ ]$	partial differentiaticn of ( ) with respect to [ ]
$(\ )^{-1}$	inverse of matrix ( )
$\sum_{(\ )}^{[\ ]}\{\ \}$	summation of { } from ( ) to [ ]
Θ	unknown parameters
$\bullet$	feasible set of unknown parameters
Γ	process noise distribution matrix
$\triangleq$	defined as
$\nu(i)$	innovations at point (i)
π	pi (3.1416)
ϕ	phi, defined by equation 49

AIRPLANE STABILITY AND CONTROL

B	speed brake deflection
CG	center of gravity
F	flap deflection
I_{xx}	moment of inertia about x axis
I_{yy}	moment of inertia about y axis

K	angle of attack vane scale factor
M	pitching moment
$M_{( )}$	pitching moment derivative
L	rolling moment
$L_{( )}$	rolling moment derivative
RPM	engine revolutions per minute
U_o	longitudinal trim airspeed
W_o	vertical trim airspeed
X	longitudinal force
$X_{( )}$	longitudinal force derivative
Z	vertical force
$Z_{( )}$	vertical force derivative
e	elevator
l	distance from CG to angle of attack vane
m	mass
n_z	normal acceleration
n	random white noise
q	pitch rate
r	yaw rate
u	longitudinal airspeed displacement from trim
w	vertical airspeed displacement from trim
z_j	perpendicular distance from C.G. to thrust line
α	angle of attack displacement from trim
α_g	gust angle of attack
$\delta_{( )}$	( ) deflection
ζ	damping ratio
ξ	thrust axis angle
θ	pitch angle

$\sigma_{(\ )}$	standard deviation of the ( ) calculated response with respect to the ( ) measured response
ϕ	roll angle
ω_c	gust break frequency
p	phugoid
sp	short period

ACKNOWLEDGEMENT

The research effort which generated this thesis was performed with the aid and direction of the Naval Air Test Center, NAS Patuxent River, Maryland, without whose cooperation this thesis could not have been completed. The author would like to specifically thank Mr. Roger Burton (Special Projects, Strike Test Directorate) who aided in the development of the thesis research topic in airframe parameter identification and for his aid and assistance in the conduct of the required research. The author would also like to thank Mr. Leonard J. Latham, Jr. (Mathematician, Scientific Applications Branch Data Reduction Section, Computer Services Division), for his able and energetic assistance during the research effort.

This thesis is the result of many hours of work not to mention the three years of study necessary to gain the engineering expertise. Through all this effort one person has offered continuous support and understanding, my wife Connie. Also my three children Terry, Chris, and Kelly have been very patient and understanding through the years of graduate study. I therefore dedicate this work, with love, to my wife Connie and my children Terry, Chris, and Kelly.

I. INTRODUCTION

A. BACKGROUND

Flight testing of military aircraft has always been a time consuming and expensive proposition. The relatively recent introduction of the new Flying Qualities Specification (MIL-F-8785B) has introduced many new parametric requirements which require that many of the aircraft airframe parameters be determined to insure specification compliance. As a result of these new requirements the Naval Air Test Center (NATC) initiated a research program to develop airframe parameter identification technology for use in flight testing Navy aircraft. This program was initiated in 1971 between the Naval Air Systems Command (NAVAIR) and NATC. At the same time the Office of Naval Research (ONR) issued a contract to Systems Control, Inc. (SCI) to advance the state-of-the-art in parameter identification. In 1973 a concentrated effort was begun by the Navy to continue the development of this new technology by forming a joint program between NATC, NAVAIR, ONR and SCI. As a result of this development a digital FORTRAN computer program, SCIDNT-I (hereafter refered to as SCIDNT) was written for NATC to extract aircraft stability and control coefficients from flight test data, Ref. 1. It was hoped that by using this computer program it would be possible to significantly reduce the flight test time in the air, and the ground data reduction.

B. PURPOSE

The purpose of this research was to develop parameter identification test methods for determining aircraft phugoid and short period characteristics from one aircraft maneuver. This research further entailed the determination of proper aircraft maneuvers/pilot inputs and detailed data analysis proceedures using the advanced maximum likelihood identification technique.

C. DESCRIPTION OF AIRPLANE

The test airplane was demonstration F-14A ship number 8 BU. NO. 157987. The airplane was essentially typical of a production F-14A airplane relative to these tests. An aircraft description is contained in Appendix A. Photographs and a three view drawing of the test airplane are shown in Appendix A , Figures 1, 2 and 3.

D. MAXIMUM LIKELIHOOD PARAMETER IDENTIFICATION THEORY

A widely used rule for choosing the sample statistic to be used in parameter estimation is called the method of maximum likelihood Ref. 2. This method, in addition to prescribing the statistic which should be used, provides an approximation of the distribution of that statistic so that approximate confidence intervals may be constructed. The method of maximum likelihood makes use of the sample-likelihood function. Assume we observe or record a set of observations on a system, whose model has p unknown parameters θ. We then can write the joint probability distribution of a random sample for any given set of values

of the parameters θ from a feasible set Θ. We then can assign a probability $p(z|\theta)$ to each outcome z. If we observe or measure the outcome of an actual experiment to be z we then would like to know which set or sets of values of θ might have resulted in these observations. This concept is contained in the likelihood function $\mathcal{L}(\theta|z)$. This function is of fundamental importance in estimation theory because of the likelihood principle of Fisher and others which states that if the system model is correct, all information about unknown parameters is contained in the likelihood function. The maximum likelihood estimator of θ is the value θ which causes the likelihood function $\mathcal{L}(\theta|z)$ to be a maximum [2].

$$\hat{\theta} = \max_{\theta \in \Theta} \mathcal{L}(\theta|z)$$

From a purely mechanical viewpoint this method can be summarized as follows:

> Find the probability density functions of the observations or measured values for all possible combinations of the unknown parameter values. Select the density function whose value is highest among all density functions at the measured values of the observations. The corresponding parameter values are the maximum likelihood estimates.

Assume θ can take three possible values: θ_1, θ_2, and θ_3. Further assume that the probability density functions of observations z for these three values of θ are as shown in Figure 1. Then, if the actual observation is z, θ_2 is the maximum likelihood estimate of θ.

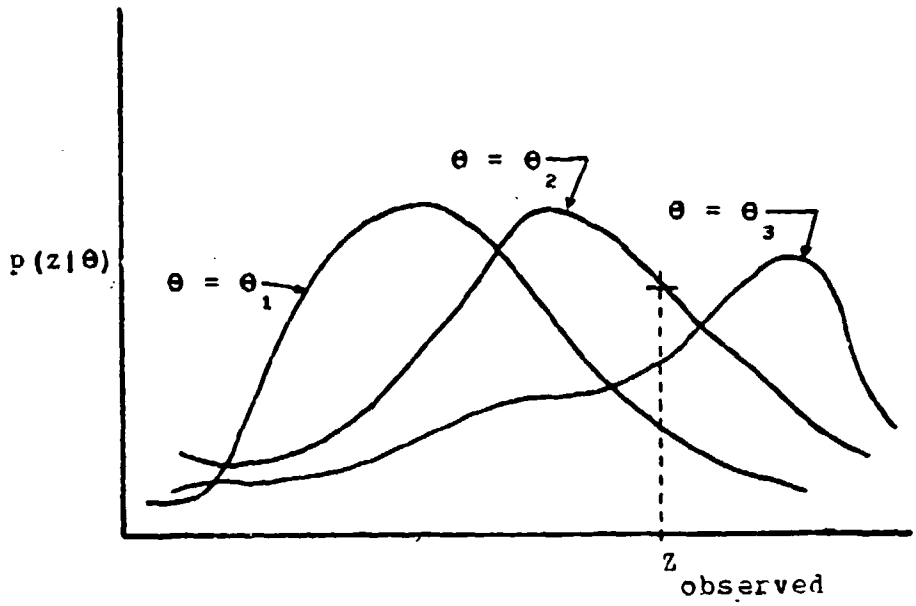

Figure 1. Maximum Likelihood Estimates

Owing to the monotonic, one-to-one relationship between the likelihood function and its logarithm, i.e. they have a maximum at the same value θ, it is more convient to work with the negative of the logarithm of the likelihood function. Starting from a priori values, the parameters are updated so that the value of the negative log-likelihood function J at the observed value of the outputs decreases continuously.

As sample statistics or functions of the observations, the estimators are, before the experiment, random variables and can be studied as such. In fact, the major advantage of maximum likelihood estimators is that their properties have been thoroughly studied and are well known, virtually independently of the particular density function under consideration. Additionally, the maximum likelihood method can be used with linear or nonlinear models in the presence of process and measurement noise. The estimator of θ is approximately normally distributed for

large n, and is asymptotically unbiased, efficient, consistent, and sufficient, [2].

The details of the maximum likelihood identification proceedure are presented in the following section.

E. MAXIMUM LIKELIHOOD IDENTIFICATION OF PARAMETERS

The derivation follows closely that presented in Ref. 3, and is presented herein for completeness and reader convenience. The initial equations will be concerned with general nonlinear systems.

Consider the general nonlinear aircraft equations of motion

$$\dot{x} = f(x, u, \theta, t) + \Gamma(\theta, t)\, w \qquad 0 \le t \le T \qquad (1)$$

$$E(x(0)) = x_o(\theta)$$

$$E\{(x(0) - x_o(\theta))(x(0) - x_o(\theta))^T\} = P_o(\theta) \qquad (2)$$

where

$x(t)$	is n x 1 state vector
$u(t)$	is l x 1 input vector
θ	is p x 1 vector of unknown parameters
$\Gamma(\theta,t)$	is n x q process noise distribution matrix
$w(t)$	is q x 1 random process noise vector

Sets of m measurements $y(t_k)$ are taken at discrete times t_k

$$y(t_k) = h(x(t_k),\ u(t_k),\ \theta,\ t_k) + v(t_k) \qquad (3)$$
$$k = 1,\ 2,\ 3,\ \ldots,\ N$$

$w(t)$ and $v(t_k)$ are Gaussian random noises [2], with the following properties

$$E(w(t)) = 0 \qquad E(v(t_k)) = 0$$

$$E(w(t)\ v^T(t_k)) = 0$$

$$E(w(t)\ w^T(\tau)) = Q(\theta,t)\ \delta(t-\tau)$$

$$E(v(t_j)\ v^T(t_k)) = R(\theta,t_j)\ \delta_{jk} \qquad (4)$$

The unknown parameters are assumed to occur in the functions f and h and in matrices Γ, Q, R, P_o, and x_o. In the following analysis, the model and the functional form of f and h is assumed known correctly.

The set of observations $y(t_1), y(t_2), \ldots, y(t_N)$ constitutes the outcome Z in this case. The likelihood function for θ, which has the same form as the probability of the outcome z for a certain value of parameters θ, is given by

$$\mathcal{L}(\theta|z) \cong p(z|\theta)$$

$$\triangleq p(y(t_1),\ y(t_2),\ \ldots,\ y(t_N)|\theta)$$

$$\mathcal{L}(\theta|z) = p(Y_N|\theta) \qquad (5)$$

where

$$Y_k = \{y(t_1),\ldots,y(t_k)\},\ k = 1, 2, \ldots, N$$

$$p(Y_N|\theta) = p(y(t_N)|Y_{N-1},\theta) \cdot p(Y_{N-1}|\theta)$$

$$= p(y(t_N)|Y_{N-1}, \theta)\ p(y(t_{N-1})|Y_{N-2}, \theta)\ p(Y_{N-2}|\theta)$$

which by successive application of Bayes rule, [2], becomes

$$p(Y_N|\theta) = \prod_{i=1}^{N} p(y(t_i)|Y_{i-1}, \theta) \qquad (6)$$

The log-likelihood function is

$$\log\ (\mathcal{L}(\theta|z)) = \sum_{i-1}^{N} \log\ \{p(y(t_i)|Y_{i-1}, \theta)\} + \text{constant} \qquad (7)$$

To find the probability distribution of $y(t_i)$ given Y_{i-1} and θ, the mean value and covariance are determined first.

$$E(y(t_i)|Y_{i-1}, \theta) \triangleq \hat{y}(i|i-1) \qquad (8)$$

The expected value or the mean is the best possible estimate of measurements at a point given the measurements up to and

including the previous point.

$$\text{cov}(y(t_i)|Y_{i-1},\theta) = E\{(y(t_i) - \hat{y}(i|i-1))(y(t_i) - \hat{y}(i|i-1))^T\}$$

$$\triangleq E\{\nu(i)\ \nu(i)^T\}$$

$$\triangleq B(i) \qquad (9)$$

$\nu(i)$ are called the innovations at point i and $B(i)$ is the innovations covariance. Since

$$y(t_i) - E(y(t_i)|Y_{i-1},\theta) = \nu(i) \qquad (10)$$

it follows that $y(t_i)$ given Y_{i-1} and θ have the same distribution as $\nu(i)$. It has been shown that as the sampling rate is increased, the innovations $\nu(i)$ tend towards having a Gaussian density. Assuming a sufficiently high sampling rate, the distribution of $\nu(i)$ and, therefore, $y(t_i)$ given Y_{i-1} and θ is Gaussian, i.e.,

$$p(y(t_i)|Y_{i-1},\theta) = \frac{\exp\left[-\frac{1}{2}\nu(i)^T B^{-1}(i)\ \nu(i)\right]}{(2\pi)^{m/2}|B(i)|^{1/2}} \qquad (11)$$

$$\log \{p(y(t_i) | Y_{i-1}, \theta)\} = -\frac{1}{2} \nu'(i)^T B^{-1}(i)\, \nu'(i)$$

$$\frac{1}{2} \log|B(i)| + \text{constant}$$

(12)

The log-likelihood function of equation (7) can be written as

$$\log (\mathcal{L}(\theta | z)) = -\frac{1}{2} \sum_{i=1}^{N} \{\nu'^T(i) B^{-1}(i)\, \nu'(i) + \log|B(i)|\} \quad (13)$$

An estimate of the unknown parameters is obtained by maximizing the likelihood function or the log-likelihood function from the feasible set of parameter values.

$$\hat{\theta} = \max_{\theta \in \Theta} \log (\mathcal{L}(\theta | z)) \quad (14)$$

$$= \max_{\theta \in \Theta} \left[-\frac{1}{2} \sum_{i=1}^{N} \{\nu'^T(i) B^{-1}(i)\, \nu'(i) + \log|B(i)|\} \right] \quad (15)$$

The log-likelihood function depends on the innovations and their covariance. To optimize the likelihood function, a way must be found for determining these quantities. Both innovations and their covariance are outputs of an extended Kalman filter.

The extended Kalman filter is conventionally divided into two parts. In the first part, called the prediction equations, the state equations and state estimate covariance equations are propagated in time from one measurement point to the next. In the second part, called the measurement update equations, the measurements and associated measurement noise covariances are used to improve state estimates. The covariance matrix is also updated at this point to reflect the additional information obtained from the measurements.

1. Prediction Equations

The state prediction is done using the equations of motion, Appendix B. Starting at time t_{i-1} with current estimate $\hat{x}(i-1|i-1)$ of the state $x(t_i)$ and the covariance $P(i-1|i-1)$, the following equations are used to find the predicted state $\hat{x}(i|i-1)$ and the associated covariance $P(i|i-1)$.

$$\frac{d}{dt}\hat{x}(t|t_{i-1}) = f(\hat{x}(t|t_{i-1}),u(t),\theta,t) \qquad (16)$$

$$\dot{P}(t|t_{i-1}) = F(t)\,P(t|t_{i-1}) + P(t|t_{i-1})\,F^{T}(t) + \Gamma Q \Gamma^{T} \qquad (17)$$

$$t_{i-1} \le t \le t_i$$

The n x n matrix F is obtained by linearizing f about the best current estimate

$$F(t) = \frac{\partial f(\hat{x}(t|t_{i-1}), u(t), \Theta, t)}{\partial \hat{x}(t|t_{i-1})} \qquad (18)$$

Using (16)~(18), we can obtain

$$\hat{x}(t_i|t_{i-1}) \triangleq \hat{x}(i|i-1)$$

and

$$P(t_i|t_{i-1}) \triangleq P(i|i-1) \qquad (19)$$

Thereafter, the measurement update equations are used.

2. Measurement Update Equations

The covariance and state estimate are updated using the measurements. The necessary relations are derived in Ref. 4, and are presented here without proof. The innovation and its covariance are

$$\nu(i) = y(i) - h(\hat{x}(i|i-1), u(t_i), \Theta, t_i) \qquad (20)$$

$$B(i) = H(i)\ P(i|i-1)\ H^T(i) + R \qquad (21)$$

where H is obtained by linearizing h,

$$H(i) = \frac{\partial h(\hat{x}(i|i-1), u(t_i, \Theta, t_i)}{\partial \hat{x}(i|i-1)} \qquad (22)$$

The Kalman gain and the state update equations are

$$K(i) = P(i|i-1)\ H^T(i)\ B^{-1}(i) \qquad (23)$$

$$\hat{x}(i|i) = \hat{x}(i|i-1) + K(i)\ \nu(i) \qquad (24)$$

Finally, P(i|i), the covariance of error in updated state, is obtained by

$$P(i|i) = (I-K(i)\ H(i))\ P(i|i-1) \qquad (25)$$

One can now return to the time update or prediction equations.

3. Optimization Procedure

Many possible numerical procedures can be used for this optimization problem. Modified Newton-Raphson or Quasilinearization have been found by experience to give quicker convergence than most procedures such as the conjugate gradient or the Davison method. The modified Newton-Raphson method is a second order gradient procedure requiring computation of first and second order partials of the log-likelihood function.

$$\frac{\partial \log\left(\mathcal{L}(\theta|z)\right)}{\partial \theta_j} = -\sum_{i=1}^{N}\left[\nu^T(i)\,B^{-1}(i)\,\frac{\partial \nu(i)}{\partial \theta_j} - \frac{1}{2}\nu^T(i)\,B^{-1}(i)\frac{\partial B(i)}{\partial \theta_j}B^{-1}(i)\,\nu(i) + \frac{1}{2}\mathrm{Tr}\left(B^{-1}(i)\,\frac{\partial B(i)}{\partial \theta_j}\right)\right] \qquad (26)$$

also

$$\frac{\partial^2 \log\left(\mathcal{L}(\theta|z)\right)}{\partial\theta_j\,\partial\theta_k} = -\sum_{i=1}^{N}\Bigg[\frac{\partial \nu^T(i)}{\partial\theta_k} B^{-1}(i)\frac{\partial \nu(i)}{\partial\theta_j}$$

$$-\frac{\partial \nu^T(i)}{\partial\theta_k} B^{-1}(i)\frac{\partial B(i)}{\partial\theta_j} B^{-1}(i)\,\nu(i)$$

$$-\frac{\partial \nu(i)}{\partial\theta_j} B^{-1}(i)\frac{\partial B(i)}{\partial\theta_k} B^{-1}(i)\,\nu(i)$$

$$+\nu^T(i) B^{-1}(i)\frac{\partial B(i)}{\partial\theta_j} B^{-1}(i)\frac{\partial B(i)}{\partial\theta_k} B^{-1}(i)\,\nu(i)$$

$$-\frac{1}{2}\mathrm{Tr}\left(B^{-1}(i)\frac{\partial B(i)}{\partial\theta_j} B^{-1}(i)\frac{\partial B(i)}{\partial\theta_k}\right)$$

$$+\frac{\partial^2 \nu(i)}{\partial\theta_j\partial\theta_k} B^{-1}(i)\,\nu(i)$$

$$-\nu^T(i) B^{-1}(i)\frac{\partial^2 B(i)}{\partial\theta_j\partial\theta_k} B^{-1}(i)\,\nu(i)$$

$$+\frac{1}{2}\mathrm{Tr}\left(B^{-1}(i)\frac{\partial^2 B(i)}{\partial\theta_j\partial\theta_k}\right)\Bigg] \qquad (27)$$

$$j,k = 1,2,\ldots,p$$

The last three terms in the equation for the second partial of the log-likelihood function involve second partials of innovation and its covariance. These terms are usually dropped which yields the second partial

approximation

$$\frac{\partial^2 \log\left(\mathcal{L}(\theta|z)\right)}{\partial\theta_j\,\partial\theta_k} = -\sum_{i=1}^{N}\left[\frac{\partial \nu^T(i)}{\partial\theta_k} B^{-1}(i)\frac{\partial \nu(i)}{\partial\theta_j}\right.$$

$$-\frac{\partial \nu^T(i)}{\partial\theta_k} B^{-1}(i)\frac{\partial B(i)}{\partial\theta_j} B^{-1}(i)\,\nu(i)$$

$$-\frac{\partial \nu(i)}{\partial\theta_j} B^{-1}(i)\frac{\partial B(i)}{\partial\theta_k} B^{-1}(i)\,\nu(i)$$

$$+\nu^T(i) B^{-1}(i)\frac{\partial B(i)}{\partial\theta_j} B^{-1}(i)\frac{\partial B(i)}{\partial\theta_k} B^{-1}(i)\,\nu(i)$$

$$\left.-\frac{1}{2}\mathrm{Tr}\left(B^{-1}(i)\frac{\partial B(i)}{\partial\theta_j} B^{-1}(i)\frac{\partial B(i)}{\partial\theta_k}\right)\right] \qquad (28)$$

From equations 20 and 21 we can obtain the gradients of innovation and its covarience for parameter θ_j as,

$$\frac{\partial \nu(i)}{\partial\theta_j} = -\left.\frac{\partial h}{\partial x}\right|_{x=\hat{x}(i|i-1)}\frac{\partial \hat{x}(i|i-1)}{\partial\theta} - \frac{\partial h}{\partial\theta} \qquad (29)$$

$$j = 1,2,\ldots,p$$
$$i = 1,2,\ldots,N$$

$$\frac{\partial B(i)}{\partial \theta_j} = \frac{\partial H(i)}{\partial \theta_j} P(i|i-1) H^T(i) + H(i) \frac{\partial P(i|i-1)}{\partial \theta_j} H^T(i)$$

$$+ H(i) P(i|i-1) \frac{\partial H^T(i)}{\partial \theta_j} + \frac{\partial R}{\partial \theta_j} \qquad (30)$$

$$j = 1,2,\ldots,p$$
$$i = 1,2,\ldots,N$$

Recursive equations can be obtained for gradients of the predicted state and its covariance. This is done in stages by using the prediction and measurement update equations of the Kalman filter. Differentiating equations 16-18 with respect to θ_j yields

$$\frac{d}{dt} \frac{\partial \hat{x}(t|t_{i-1})}{\partial \theta_j} = \frac{\partial f(\hat{x}(t|t_{i-1}), u(t), t, \theta)}{\partial \theta_j}$$

$$+ \frac{\partial f(\hat{x}(t|t_{i-1}), u(t), t, \theta)}{\partial \hat{x}(t|t_{i-1})} \cdot \frac{\partial \hat{x}(t|t_{i-1})}{\partial \theta_j}$$

$$\frac{\partial \hat{x}(0|0)}{\partial \theta_j} = \frac{\partial x_o(\theta)}{\partial \theta_j} \qquad (31)$$

$$\frac{d}{dt}\frac{\partial P(t|t_{i-1})}{\partial \theta_j} = \frac{\partial F(t)}{\partial \theta_j} P(t|t_{i-1}) + F(t)\frac{\partial P(t|t_{i-1})}{\partial \theta_j}$$

$$+ \frac{\partial P(t|t_{i-1})}{\partial \theta_j} F^T(t) + P(t|t_{i-1})\frac{\partial F^T}{\partial \theta_j}$$

$$+ \frac{\partial \Gamma}{\partial \theta_j} Q \Gamma^T + \Gamma \frac{\partial Q}{\partial \theta_j} \Gamma^T + \Gamma Q \frac{\partial \Gamma^T}{\partial \theta_j}$$

$$\frac{\partial P(0|0)}{\partial \theta_j} = \frac{\partial P_o(\theta)}{\partial \theta_j} \qquad t_{i-1} \leq t \leq t \qquad (32)$$

$$\frac{\partial F(t)}{\partial \theta_j} = \frac{\partial^2 f(\hat{x}(t|t_{i-1}), u(t), \theta, t)}{\partial \theta_j \partial \hat{x}(t|t_{i-1})} \qquad (33)$$

$$j = 1,2,\ldots,p$$

The sensitivity functions, used in the SCIDNT integration routines, are updated at measurement points by differentiating equations 22 - 25 with respect to θ_j.

$$\frac{\partial H(i)}{\partial \theta_j} = \frac{\partial^2 h(\hat{x}(i|i-1), u(t_i), \theta, t_i)}{\partial \theta_j \partial \hat{x}(i|i-1)} \qquad (34)$$

$$\frac{\partial K(i)}{\partial \theta_j} = \frac{\partial P(i|i-1)}{\partial \theta_j} H^T(i)\ B^{-1}(i)$$

$$+ P(i|i-1) \frac{\partial H^T(i)}{\partial \theta_j} B^{-1}(i)$$

$$- P(i|i-1)\ H^T(i)\ B^{-1}(i) \frac{\partial B(i)}{\partial \theta_j} B^{-1}(i) \quad (35)$$

$$\frac{\partial \hat{x}(i|i)}{\partial \theta_j} = \frac{\partial \hat{x}(i|i-1)}{\partial \theta_j} + \frac{\partial K(i)}{\partial \theta_j} v'(i) + K(i) \frac{\partial v'(i)}{\partial \theta_j} \quad (36)$$

$$\frac{\partial P(i|i)}{\partial \theta_j} = (I - K(i)\ H(i)) \frac{\partial P(i|i-1)}{\partial \theta_j}$$

$$- \frac{\partial K(i)}{\partial \theta_j} H(i)\ P(i|i-1)$$

$$- K(i) \frac{\partial H(i)}{\partial \theta_j} P(i|i-1) \quad (37)$$

$$j = 1,2,3,\ldots,p$$

The negative of the matrix of second partials of the log-likelihood function is called the information matrix M. The step size $\Delta\theta$ for parameter estimates is given by

$$\Delta\theta = M^{-1} \frac{\partial \log (\mathcal{L}(\theta|z)}{\partial \theta} \quad (38)$$

The information matrix provides a lower bound on parameter estimate covariances, i.e.,

$$E(\theta-\hat{\theta})\ (\theta-\hat{\theta})^{T} \geq M^{-1} \qquad (39)$$

This is the Cramer-Rao lower bound. The maximum likelihood estimates approach this bound asymptotically.

4. Linear Systems

In a linear system, the functions f and h are defined as

$$f(x,u,\theta,t) \triangleq F(\theta,t)\,x + G(\theta,t)\,u$$

and $$h(x,u,\theta,t) \triangleq H(\theta,t)\,x + D(\theta,t)\,u \qquad (40)$$

For the linear case, it has been shown that if the model is correct, the innovations are white and have Gaussian density at the true values of the parameters. The assumption of fast sampling rate is, therefore, not necessary,

The basic algorithm for solution of the linear case, is the same, however, some of the equations can now be simplified. The equivalence between F(t) and H(i) of (18) and (22) and F(θ,t) and $H(\theta,t_i)$ of (40) is obvious. Equations (16) and (20) now become

$$\frac{d}{dt}\,\hat{x}(t|t_{i-1}) = F(\theta,t)\;\hat{x}(t|t_{i-1}) + G(\theta,t)\;u(t) \qquad (41)$$

and

$$\nu(i) = y(i) - H(\theta,t_i)\;\hat{x}(i|i-1) - D(\theta,t_i)\;u(t_i) \qquad (42)$$

Equations (29) and (31) can be written as

$$\frac{\partial \nu(i)}{\partial \theta_j} = - H(\theta,t_i)\,\frac{\partial \hat{x}(i|i-1)}{\partial \theta_j} - \frac{\partial H(\theta,t_i)}{\partial \theta_j}\,\hat{x}(i|i-1) - \frac{\partial D(\theta,t_i)}{\partial \theta_j}\,u(t_i) \qquad (43)$$

and

$$\frac{d}{dt}\,\frac{\partial \hat{x}(t|t_{i-1})}{\partial \theta_j} = F(\theta,t)\,\frac{\partial \hat{x}(t|t_{i-1})}{\partial \theta_j} + \frac{\partial F(\theta,t)}{\partial \theta_j}\,\hat{x}(t|t_{i-1}) + \frac{\partial G(\theta,t)}{\partial \theta_j}\,u(t) \qquad (44)$$

All other equations remain the same.

There is a considerable reduction in the computation requirement for time-invariant linear systems. In this case, matrices F, G, H, D, Γ, Q and R and their derivatives with respect to the parameters are constant.

5. Time Invariant Linear Systems In Statistical Steady State

In many aircraft applications, the Kalman filter is in steady state for the duration of the experiment. This occurs when the Kalman filter is in operation for a sufficiently long time and the process and measurement noise covariances are constant. The Kalman gain and the innovations and the state covariances approach constant values. The time update and measurement update equations for the covariances are

$$\frac{d}{dt}P(t|t_{i-1}) = FP(t|t_{i-1}) + P(t|t_{i-1})F^T + \Gamma Q \Gamma^T \qquad (45)$$

$$K = P(i|i-1)H^T B^{-1} \qquad (46)$$

$$B = HP(i|i-1)H^T + R \qquad (47)$$

$$P(i|i) = (I-KH)\ P(i|i-1) \qquad (48)$$

By definition of the steady state

$$P(i-1|i-1) = P(i|i)$$

Therefore, from (45)

$$P(i|i-1) = e^{F\,\Delta t}\, P(i-1|i-1)\, e^{F^T \Delta t} + \int_{t_{i-1}}^{t_i} e^{F(t_i-\tau)}\, \Gamma Q \Gamma^T e^{F^T(t_i-\tau)}\, d\tau$$

$$= e^{F\,\Delta t}\, (I-KH)\, P(i|i-1)\, e^{F^T \Delta t} + \int_{t_{i-1}}^{t_i} e^{F(t_i-\tau)}\, \Gamma Q \Gamma^T e^{F^T(t_i-\tau)}\, d\tau$$

$$\triangle\ \phi(\Delta t)\, (I-KH)\, P(i|i-1)\, \phi(\Delta t) + Q'$$

$$= \phi(\Delta t)\, (P(i|j-1) - KBK^T)\, \phi(\Delta t) + Q' \qquad (49)$$

Using (46), (47) and (49), we can solve for $P(i|i-1)$ and then find K and B. Also, it can be shown that

$$\frac{\partial P}{\partial \theta_j} = A_1 \frac{\partial P}{\partial \theta_j} A_1^T + A_2 - \phi P A_3 P \phi^T \qquad (50)$$

$$\frac{\partial K}{\partial \theta_j} = (I-KH) \frac{\partial P}{\partial \theta_j} H^T (HPH^T + R)^{-1} + A_2 \qquad (51)$$

$$\frac{\partial B}{\partial \theta_j} = \frac{\partial H}{\partial \theta_j} P H^T + H \frac{\partial P}{\partial \theta_j} H^T + H P \frac{\partial H^T}{\partial \theta_j} + \frac{\partial R}{\partial \theta_j} \qquad (52)$$

where

$$A_1 = \phi(I-KH)$$

$$A_2 = \frac{\partial \phi}{\partial \theta_j} (I-KH) P \phi^T + \phi (I-KH) P \frac{\partial \phi^T}{\partial \theta_j}$$

$$- \phi K \frac{\partial H}{\partial \theta_j} P \phi^T + \frac{\partial Q'}{\partial \theta_j}$$

$$A_3 = \frac{\partial H^T}{\partial \theta_j} B^{-1} H + H^T B^{-1} \frac{\partial H}{\partial \theta_j} P H^T$$

$$+ H P \frac{\partial H^T}{\partial \theta_j} + \frac{\partial R}{\partial \theta_j} B^{-1} H \qquad (53)$$

$$P \triangle P(i|i-1)$$

Thus, it is possible to solve for $\frac{\partial P}{\partial \theta_j}$ using (50) and then find $\frac{\partial K}{\partial \theta_j}$ and $\frac{\partial B}{\partial \theta_j}$ from (51) and (52). Equation (50) is a linear equation in $\frac{\partial P}{\partial \theta_j}$ and the coefficient of the unknown matrix does not depend on the parameter

θ_j. Thus, the sensitivity of the state covariance matrix can be determined very quickly for all parameters. Once the sensitivity of P, K and B for unknown parameters is determined, only state sensitivity equations need to be updated. The computation of state sensitivity functions can be reduced to many fewer equations.

An approximation simplifies the problem further. The unknown parameters are defined to include elements in K and B matrices instead of Q and R. Optimizing the log-likelihood function for parameters in B gives

$$\hat{B} = \frac{1}{N} \sum_{i=1}^{N} \nu(i) \; \nu^T(i) \qquad (54)$$

The gradient of the log-likelihood function with respect to other unknown parameters is

$$\frac{\partial \, \mathrm{Log}(\mathcal{L}(\theta|z))}{\partial \theta_j} = -\sum_{i=1}^{N} \nu^T(i) \; \hat{B}^{-1} \frac{\partial \nu(i)}{\partial \theta_j} \qquad (55)$$

The sensitivity of innovations to parameters is determined using the following recursive equations

$$\frac{d}{dt} \hat{x}(t|t_{i-1}) = F\hat{x}(t|t_{i-1}) + Gu(t)$$

$$\frac{d}{dt}\frac{\partial \hat{x}(t|t_{i-1})}{\partial \theta_j} = \frac{\partial F}{\partial \theta_j}\hat{x}(t|t_{i-1}) + F\frac{\partial \hat{x}(t|t_{i-1})}{\partial \theta_j} + \frac{\partial G}{\partial \theta_j}u(t)$$

$$j = 1,2,\ldots,p \qquad t_{i-1} \le t \le t_i \qquad (56)$$

$$\nu(i) = y(i) - H\hat{x}(i|i-1) - Du(t_i)$$

$$\hat{x}(i|i) = \hat{x}(i|i-1) + K\nu(i) \qquad (57)$$

$$\frac{\partial \nu(i)}{\partial \theta_j} = -\frac{\partial H}{\partial \theta_j}\hat{x}(i|i-1) - H\frac{\partial \hat{x}(i|i-1)}{\partial \theta_j} - \frac{\partial D}{\partial \theta_j}u(t_i) \qquad (58)$$

$$\frac{\partial \hat{x}(i|i)}{\partial \theta_j} = \frac{\partial \hat{x}(i|i-1)}{\partial \theta_j} + \frac{\partial K}{\partial \theta_j}\nu(i) + K\frac{\partial \nu(i)}{\partial \theta_j}$$

$$j = 1,2,\ldots,p$$

Note that

$$\frac{\partial K}{\partial \theta_j} = 0 \quad \text{if } \theta_j \text{ is not an element of K matrix}$$

$$= I_{j'k'} \quad \text{if } \theta_j \triangleq K_{j'k'} \qquad (59)$$

where $I_{j'k'}$ is a matrix of all zeroes except a 1 at the j', k' position.

This approximation simplifies the optimization considerably. However, this usually leads to an overparameterized model. In other words, once K and B are determined, it is not possible to find any corresponding Γ, Q and R which have the desired (known a priori) structure. A good estimate of elements in Γ, Q and R matrices can be obtained by a least-squares type approach. The fit to the observed data is better than with true values of parameters but the parameter estimates do not have minimum variance. This approximation is not good in aircraft application where the structure of Q and R is known fairly well, but is excellent where there are many process noise sources and the characteristics of both Q and R are relatively unknown (e.g., economic systems).

6. Maximum Likelihood With No Process Or Measurement Noise

The maximum likelihood method can be simplified when either process noise or measurement noise are absent. Assuming no process noise we can proceed as follows.

If the process noise is zero and initial states are known perfectly, i.e., w(t) and P(0) are zero, the covariance of the error in the predicted state is also zero. It is clear from (23) that the Kalman gains are zero. The innovations are the output error, i.e.,

$$\nu(i) = y(i) - h(x(t_i), u(t_i), \theta, t_i) \qquad (60)$$

and the innovation covariance is (21)

$$B(i) = R \qquad (61)$$

the log-likelihood function is,

$$\log\left(\mathcal{L}(\theta|z)\right) = -\frac{1}{2}\sum_{i-1}^{N} \nu^{T}(i)\, R^{-1}\nu(i) + \log|R| \qquad (62)$$

which on optimizing for unknown parameters in R yields

$$\hat{R} = \frac{1}{N}\sum_{i=1}^{N} \nu(i)\ \nu^{T}(i) \qquad (63)$$

The equality in (63) holds only for those elements of R which are not known a priori. For instance, even if R is known to be diagonal, the right hand side matrix will not be diagonal in general, but the off-diagonal terms should be ignored before they are equated to R. Using (63) in (62) we obtain

$$\log\left(\mathcal{L}(\theta|z)\right) = -\frac{1}{2}\sum_{i=1}^{N} \nu^{T}(i)\, R^{-1}\ \nu(i) + \text{constant} \qquad (64)$$

The optimizing function is the same as that for the output error method except that the measurement noise covariance matrix is determined using (63) and is used as the weighting matrix in the criterion function. In the output error method, the measurement noise is assumed known and the weighting function is arbitrary.

The first and second derivatives of the log-likelihood function with respect to unknown parameters are

$$\frac{\partial}{\partial \theta_j} \log(\mathcal{L}(\theta|z)) = -\sum_{i=1}^{N} \nu^T(i)\ \hat{R}^{-1}\ \frac{\partial \nu(i)}{\partial \theta_j} \qquad (65)$$

$$\frac{\partial^2 \log(\mathcal{L}(\theta|z))}{\partial \theta_j\ \partial \theta_k} = -\sum_{i=1}^{N}\left[\frac{\partial \nu^T(i)}{\partial \theta_k}\ \hat{R}^{-1}\ \frac{\partial \nu(i)}{\partial \theta_j} + \nu^T(i)\ \hat{R}^{-1}\ \frac{\partial^2 \nu(i)}{\partial \theta_j \partial \theta_k}\right] \qquad (66)$$

The terms in the second derivative are approximated as

$$\frac{\partial^2 \log(\mathcal{L}(\theta|z))}{\partial \theta_j\ \partial \theta_k} = -\sum_{i=1}^{N}\left[\frac{\partial \nu^T(i)}{\partial \theta_k}\ \hat{R}^{-1}\ \frac{\partial \nu(i)}{\partial \theta_j}\right] \qquad (67)$$

With no measurement noise we can proceed as follows. If all states are measured with no noise, the covariance of the error in state estimates is zero at the

beginning of any time update,

$$P(i-1|i-1) = 0$$

$$\text{and} \qquad \hat{x}(i-1|i-1) = x(i-1) \tag{68}$$

It is easy to show in this case that for fast sampling the log-likelihood function is quadratic in the difference between measure values of $\dot{x}$ and $f(x,u,\theta,t)$. The method reduces to the equation error method, the weight W being chosen as

$$W = \frac{1}{T}\int_0^T (\dot{x} - f(x,u,\theta,t))\ (\dot{x} - f(x,u,\theta,t))^T dt \tag{69}$$

Thus, the maximum likelihood method and equation-error methods are equivalent except for the technique for choosing the weighting matrix.

F. AIRCRAFT PARAMETER IDENTIFICATION USING THE MAXIMUM LIKELIHOOD METHOD

In applying the maximum likelihood theory it is necessary to consider the aircraft equations of motion in discrete form. It was assumed that the structure of the model was known. The vector of unknown parameters from $x(0)$, ϕ, G, Γ, H, Q, and R was denoted by θ. The

problem, therefore, was to identify θ using the maximum likelihood method. In constructing the problem it was further assumed that the aircraft which had been flying for some time was in a steady state condition, and process noise (wind gust effects) was not present.

In the computer implementation, the negative log-likelihood function was minimized using a Gauss-Newton gradient procedure. A least squares routine was utilized to provide approximate airframe parameter start-up values. Additionally the results of the SCIDNT computer program were utilized to obtain frequency and damping.

G. SCOPE OF RESEARCH

Research was limited to the longitudinal case since both available computer and research time were limited. Although additional data were desired, the project airplane was substantially damaged by fire and was removed from further test activity. Further data gathering with the F-14A airplane was, therefore, not possible. Specific longitudinal stability derivatives identified are given in the Results and Discussion section. There were no airplane flight restrictions which affected the test methods or limited the scope of research. The research was limited to establishing base line data for the short period and phugoid modes and thence to determine the feasibility of identifying these modes simultaneously.

H. METHOD OF TESTS

In general test proceedures were in accordance with those contained in the U. S. Naval Test Pilot School Fixed Wing Stability and Control Manual, Ref 5. There were, however, some non-standard test techniques utilized in

exciting the desired airplane modes. The short period mode was excited by the standard doublet method and additionally by applying a sinusoidal control input at varying frequencies. The phugoid mode was excited by the Delta Airspeed method in all cases, [5].

In exciting the phugoid and short period modes simultaneoulsy, a combination of standard test techniques were utilized. The "simultaneous" technique consisted of establishing the airplane in a phugoid maneuver and during the first quarter cycle of the maneuver applying a doublet input to excite the short period mode.

The data system utilized within the airplane was specifically designed to be compatible with the Naval Air Test Center Real-Time Telemetry Processing System (RTPS). A brief description of the airplane and ground data systems is presented in Appendix C. Data reduction was performed on the RTPS Xerox Sigma 9 computer in the batch processing mode. Raw airplane data were converted to an Engineering Unit tape and used as input to the digital parameter identification program (SCIDNT). In addition a least squares parameter identification routine was utilized to generate parameter start up values for SCIDNT. This least squares routine extracted a set of approximate stability derivatives by minimizing the error between the model and actual airplane state vector time histories.

II. RESULTS AND DISCUSSION

A. SHORT PERIOD AIRFRAME PARAMETER IDENTIFICATION

1. Airplane Test Conditions

Initial trimmed test conditions for each control input are presented in Table I. Prior to each control input the airplane was trimmed for steady state "hands off" flight [5].

	Altitude (ft HPC)	MACH	CG (% MAC)	Loading
Sine Wave Input	29 925	.6149	11.18	B (1)
Doublet Input	30 503	.6289	10.985	B

(1). Four Sparrow III missiles (AIM-7) on stations 3, 4, 5 and 6

Table I. Short Period Test Conditions

2. Method Of Investigation

The airplane model equations used were those shown in Appendix B. In order to isolate the short period mode from the longitudinal equations of motion the state vector parameters α, q, and θ were made insensitive to u. This was accomplished simply by fixing X_α, X_u, X_q, Z_u, M_u and X_{θ_e}

equal to zero and not identifying any of them. This equation modification resulted in the clasical short period approximation Ref. 6.

To provide SCIDNT with approximate airframe parameter start-up values,the least squares routine was utilized. For the short period case the least squares start up values were very good, a comparison of a typical set of least squares parameters and the final SCIDNT parameter values is shown in Table II.

	Z_{α}	Z_q	M_{α}	M_q	Z_{δ_e}	M_{δ_e}
Least Squares	-.4909	0.9624	-1.78	-.9085	0.210	6.09
SCIDNT	-.4903	0.9805	-1.95	-.795	0.278	5.542

Table II. Comparison of Least Squares Parameter Values and SCIDNT Parameter Values

In actual practice, however, airplane data was recorded in long bursts which usually included three or more maneuvers , executed with near identical initial conditions. As a result once a set of start up values were determined for a given test condition it was unnessary to determine a set of start up values for other like maneuvers.

The actual parameter identification proceedure , for the short period mode, was relatively simple once familiarity with the digital program was attained. Upon obtaining a set of "reasonable" initial parameter estimates, all six short period parameters were estimated in an iterative fashion. Here "reasonable" denotes proper parameter sign and magnitude. Each computer run was made with the number of iterations and step cuts both initialized at ten. During a given iteration the program attempted to

minimize the likelihood function. If the likelihood function increased, a series of step cuts would be taken until the likelihood function again decreased or the maximum number of step cuts were exceeded. The program would then continue to iterate until the desired number of iterations/step cuts were reached. Due to program logic one more step cut than requested was executed. For the short period mode, however, convergence was obtained early in program execution. In general, iterations conducted with doublet control input data converged very quickly and began executing step cuts until the allowable number was exceeded. Figure 2 shows the change in the likelihood function during iteration for a doublet input. Program convergence had been essentially reached by the fourth iteration at which time a series of step cuts were made.

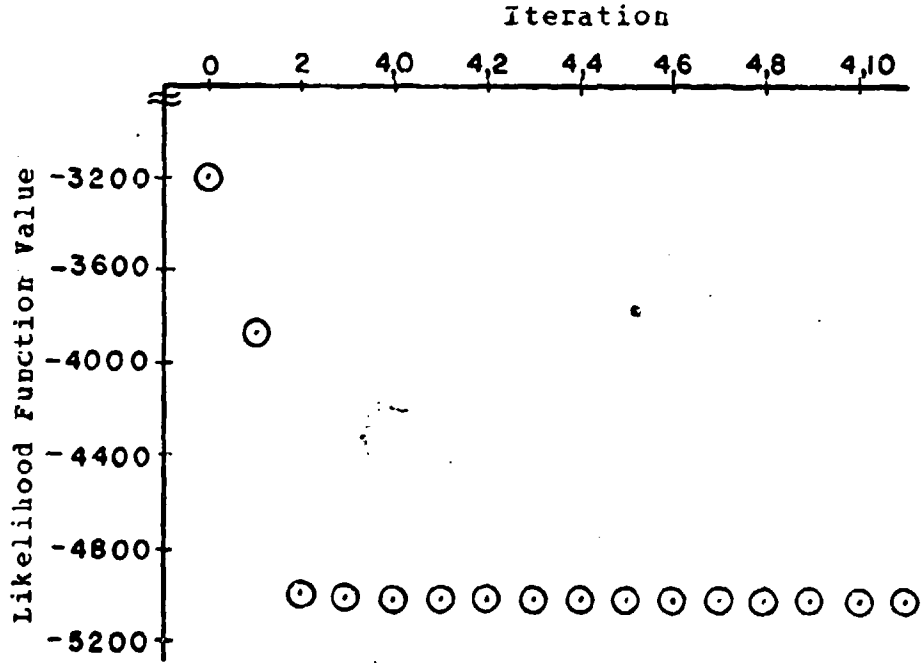

Figure 2. Likelihood Function Change During Iteration For Doublet Input

The convergence characteristics using sinusoidal input data were somewhat different. During the program

iteration the likelihood function continuously decreased and no step cuts were taken, Figure 3. Program convergence for this case was evidenced by a leveling out of the likelihood function, but not until the eighth iteration. It was felt that since the data length for the sinusoidal input was longer than the short period data length the larger number of iterations until program convergence was not abnormal.

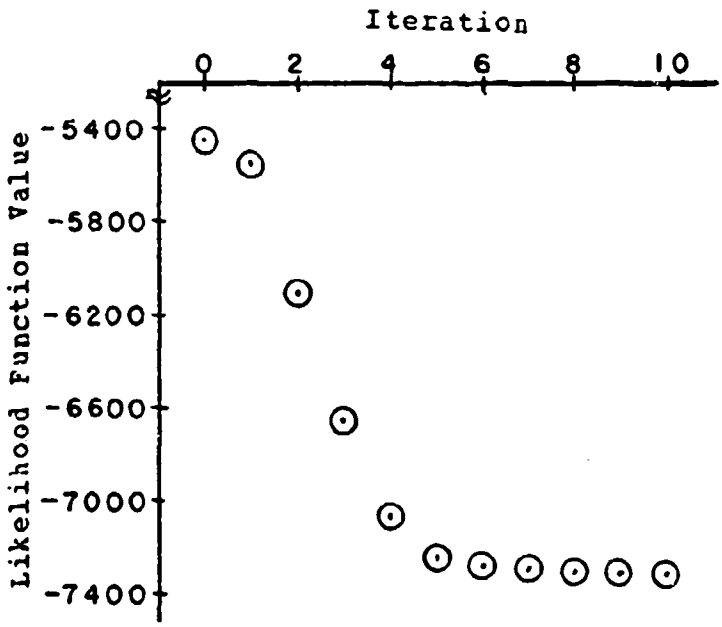

Figure 3. Likelihood Function Change During Iteration For Sinusoidal Input

After convergence was obtained for the parameter estimates, the Angle Of Attack Scale Factor (K_α) was determined. K_α was a scaling factor in the angle of attack measurement equation, Appendix B. In estimating K_α two terms in the model were actually affected, K_α itself and the variable ($l_\alpha K_\alpha / U$) which was used to multiply q in the measurement equation. Since, in essence, two terms were being estimated a modified form of parameter estimation was utilized. In the term ($l_\alpha K_\alpha / U$) the value of K_α was initially set to 1.0 and the single term K_α was

determined. This new value of K_{α} was then substituted into the term ($l_{\alpha} K_{\alpha} /U$) and again a set of iterations were performed to determine an updated K_{α}. This method of iteration was continued until there was essentially no change in K_{α}, at which time the value was said to have converged. In most cases only two iterations were required to obtain a converged K_{α}.

Upon determining a value for K_{α}, a final set of iterations were performed to determine values for Z_o, X_o, M_o, θ_o. At this point, the short period mode time history fits were nearly identical and the estimate statistics indicated a high degree of confidence. Attempts at further iterations to improve the estimates resulted in using a lot more computer time, with very little improvement. Therefore, the procedure utilized to estimate the short period mode was to first estimate the short period parameters, second estimate K_{α}, and finally, estimate the initial values.

3. Data Analysis

Data from typical short period estimation runs for a doublet and sinusoidal input are presented in Tables III and IV. Typical short period time history fits are presented in Appendix D Figures 1 and 2, for the doublet and sinusoidal inputs respectfully. It should be noted that the scales for the short period time histories are different for the doublet and sinusoidal inputs. Furthermore, since the estimated stability derivatives were in dimensional form the actual derivative values differed slightly from maneuver to maneuver.

The data obtained with the doublet input in most all cases converged to believable derivative estimates, i.e., expected sign and magnitude, with favorable iteration statistics. For example, refering to Table III, the value of M_{α} was -1.844 with a standard deviation of 0.0061 and a final step size of -0.0146 which is significantly lower in

magnitude than the estimated parameter. From probability theory we can say that the probability is 99.74% that the value of M_{α} is -1.844 ±0.0183 which is well within acceptable engineering tolerances. This same analysis was carried out for the other estimated derivatives with similar results.

Derivatives	Z_{α}	Z_q	M_{α}	M_q	Z_{θ_e}	M_{θ_e}
Estimate	-.4138	1.099	-1.844	-.826	0.1628	5.098
Standard Deviation	0.0024	0.0038	0.0061	0.0037	0.0055	0.0104
Parameter Step Size	-.0006	-.012	-.0146	-.0001	0.0143	0.028
Eigenvalue Spread			1.28×10^6			
Likelihood Function Value			-5.1×10^3			
Time History Matches	$\sigma_{\alpha} = 0.00396$		$\sigma_u = 0.564$		$\sigma_q = 0.0039$	
	$\sigma_{\theta} = 0.0043$		$\sigma_{n_z} = 2.33$			

Table III. SCIDNT Estimates of Longitudinal Short Period Stability Derivatives Using a Doublet Input

The eigenvalue spread, that is, the difference between the largest eigenvalue and the smallest eigenvalue of the information matrix, was 1.28×10^6 which was less than the maximum spread allowed by SCIDNT (10^{10}). All parameters converged indicating no identifiability problems, and the eigenvalue spread was therefore not considered significant. The likelihood function value was a large negative number which converged rapidly (Figure 2), further indicating no identifiability problems.

As a final check of stability derivative correctness a series of time history fits were constructed. In constructing these plots both the model and airplane were excited with the same control input and the airplane time history plots superimposed on the same scale. The time history fit for the doublet input was, in general, very good, with the difference between the measured value and estimated value within the instrumentation measurement error tolerances Ref. 7.

Referring to Table IV, it can be seen that typically the estimated derivatives using a sinusoidal input converged to appropriate (sign and magnitude) stability derivative values.

Derivatives	Z_α	Z_q	M_α	M_q	Z_{δ_e}	M_{δ_e}
Estimate	-.4303	1.1229	-2.007	-.7615	0.1532	5.2274
Standard Deviation	0.0042	0.0061	0.013	0.007	0.0045	0.0181
Parameter Step Size	0.0007	-.0016	-.0043	-.0061	-.0037	0.0332
Eigenvalue Spread			1.67×10^5			
Likelihood Function Value			-7.323×10^3			
Time History Matches	$\sigma_\alpha = 0.00533$		$\sigma_u = 0.9$		$\sigma_q = 0.006$	
	$\sigma_\theta = 0.01$		$\sigma_{n_z} = 2.32$			

Table IV. SCIDNT Estimates of Longitudinal Short Period Stability Deravitives Using A Sinusoidal Input

In general, however, the parameter standard deviations and step sizes were not as favorable as those obtained with the doublet input for these two examples. It was

possible, however, to select another pair of maneuvers and reach the opposite conclusion, ie. sinusoidal input more favorable. Since all parameter estimates for both the doublet and sinusoidal inputs converged it was concluded that the slight difference in statistical data was not significant. If a determination as to which control input to use were required, it was felt that the primary consideration would be ease of pilot input. If an autopilot device were available which could input the sinusoid then this input should be used, however, with no autopilot system installed the doublet input would provide excellent results.

A consistent problem that occured throughout the research was concerned with the initial conditions prior to the control input. If the initial condition of the airplane was not stabilized prior to the control input or if a data burst was taken in the middle of a control input, no time history match was possible. According to theory it is possible to extract the airframe parameters at any time during a maneuver, this, however did not appear to be true. Figure 3 Appendix D shows the results of estimating the parameters starting from non-zero initial conditions. This time history fit was generated after all iterations on both parameters and initial conditions were completed. The parameter estimates did not converge and the most powerful derivative, M_{α}, was much larger in magnitude than any other estimates with a value of -3.7. These results occured any time an attempt was made to start SCIDNT from an initial condition other than steady state. It was concluded that, within the scope of this research, meaningful parameter estimates were only obtainable when started from an initial steady state condition.

A comparison of short period characteristics obtained from Navy Preliminary Evaluation (NPE) data and those determined by SCIDNT is presented in Table V.

Description	Damping Ratio ζ_{sp}	Frequency $\omega_{n_{sp}}$ (rad/sec)
NPE	0.35	1.49
SCIDNT-Doublet	0.403	1.54
SCIDNT-Sinusoidal	0.371	1.61

Table V. Comparison of Longitudinal Short Period Characteristics

It was concluded that, within the scope of this research, the parameter identification program SCIDNT was easy and straightforward to use in determining the short period mode. In addition, it was concluded that it was not possible to obtain accurate estimates when starting from non-steady state initial conditions.

B. PHUGOID AIRFRAME PARAMETER IDENTIFICATION

1. Airplane Test Conditions

Initial trimmed test conditions for the phugoid maneuver are presented in Table VI. Prior to the control input the airplane was trimmed for steady state "hands off" flight [5].

	Altitude (Ft HPC)	MACH	CG (% MAC)	Loading
Phugoid Input	30 055	0.614	10.94	B

Table VI. Phugoid Test Conditions

2. Method Of Investigation

The airplane model equations used were those shown in Appendix B. The derivitives X_{α} and X_{δ_e} were fixed at zero values since their effect on the phugoid was small. Additionally, it was felt, fixing these terms would facilitate the identification of the dominant phugoid terms. Finally from Appendix B it can be seen that the term X'_q was defined as $(X_q - \alpha_o U_o)$ and therefore due to its relatively large size was approximated by $\alpha_o U_o$ and fixed. The parameters which were identified during the pure phugoid maneuver were therfore, Z_u, X_u, and M_u.

Since there was no short period input during the pure phugoid maneuver it was not possible to effectively identify the short period parameters. Additionally the program solution diverged without a set of predefined short period parameters and it was necessary to obtain parameters from a prior run. A set of short period parameters were, therefore, obtained from a previous identification run and fixed throughout the phugoid parameter identification runs.

In an attempt to provide SCIDNT with approximate airframe parameter start-up values the least squares routine was utilized. For the phugoid case the least squares start up values were unusable. For example, least squares values for X_{α} was -2.6697 and X_{δ_e} was -240.5, both of which are terms of small absolute value. As an additional check, the least squares parameter estimates were used to generate a set of time histories. For these time historys the standard deviation of airspeed and normal acceleration was 49.12 ft/sec and 5.44 ft/sec^2 respectively. Therefore, since the least squares routine did not provide acceptable start-up

values the identified parameters were set initally to zero for the first SCIDNT iteration. Further attempts to obtain phugoid start up values for SCIDNT from the least squares routine proved futile and its use was discontinued for the phugoid case.

The version of SCIDNT utilized for this investigation would accept a maximum of 500 data samples per run. Since the phugoid period was approximately 100 sec a data burst recorded at 20 samples per second (SPS) would only include the first 25 sec of the maneuver. This time span was obviously acceptable for the short period mode but clearly unacceptable during a phugoid maneuver. An attempt was therefore, made to utilize data at 2 and 5 SPS to include as much of the phugoid maneuver as possible. This data was from the same maneuver with data tapes recorded at 2 and 5 SPS.

Although the 2 SPS data would provide a longer phugoid time span in theory, the program exhibited severe instabilities during the control input and therefore only the latter portion of the data burst was usable. It was strongly suspected that these instabilities were due to the unusually rough control inputs.

The actual parameter identification procedure for the phugoid mode was somewhat different than that utilized during the short period investigation. The short period stability derivatives were obtained from a run whose initial conditions most closely approximated those of the phugoid run. These short period parameters were then fixed as constants during the phugoid iterations. Computer runs were made with the number of iterations and step cuts both initialized at ten. The program would then continue to iterate until the desired number of iterations/step cuts were completed. For both the 5 SPS and 2 SPS data convergence was obtained prior to executing the full 10 iterations. Iterations conducted with phugoid data recorded at 2 SPS appeared to converge very quickly and began

executing step cuts until the allowable number was exceeded. As in the short period case the program executed one step cut more than requested. Figure 4. presents the change in the likelihood function during iteration using phugoid data recorded at 2 SPS. The program converged to its "best" solution by the third iteration at which time the step cuts were executed.

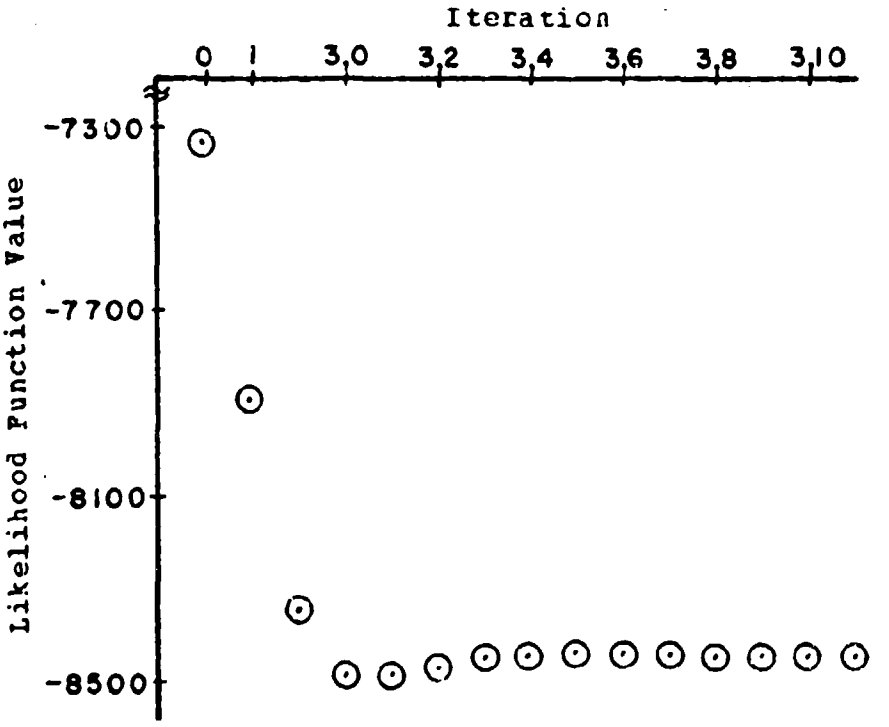

Figure 4. Likelihood Function During Iteration Using 2 SPS

Note that although the program had apparently converged at the third iteration the value of the likelihood function decreased until the fourth step cut. The function value then remained essentially constant throughout the remaining step cuts.

The convergence characteristics using data recorded at 5 SPS were somewhat different, Figure 5.

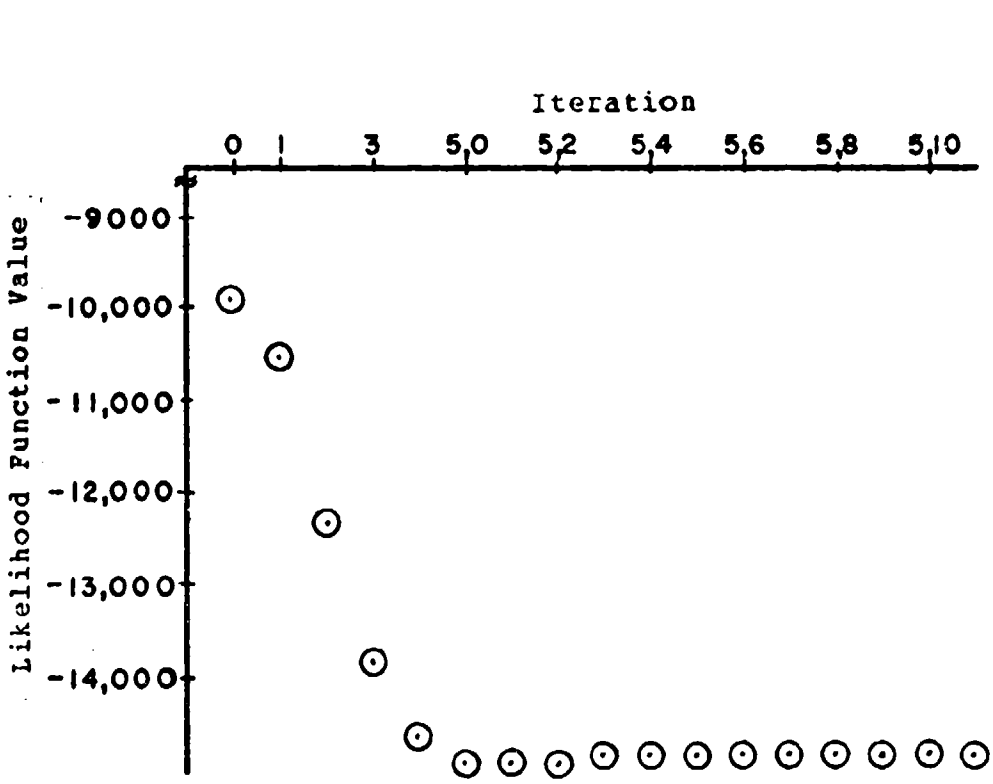

Figure 5. Likelihood Function During Iteration Using 5 SPS

It should be noted, however, that the scales are different for each plot. The program had essentially converged at the fifth iteration, at which time the program executed step cuts. Note that the likelihood function values decrease using 5 SPS data, and were essentially the same using the 2 SPS data. However, the time history matches for each set of data were significantly different. The angle of attack scale factor (K_{α}) was not estimated since the value of K_{α} from the short period data was utilized. After convergence was obtained for the parameter estimates a final set of iterations was performed to estimate values for Z_o, X_o, M_c, θ_o and the three phugoid parameters

simultaneously. At this point, the phugoid time history fits were acceptable for the 5 SPS data and clearly unacceptable using the 2 SPS data. Further attempts to improve the estimates and time histories resulted in using a lot more computer time with no improvement.

3. Data Analysis

Data from phugoid estimation runs using 2 SPS and 5 SPS are presented in Tables VII and VIII respectfully. Phugoid time history fits are presented in Appendix D Figures 4 and 5 for 2 and 5 SPS respectfully. It should be noted that the scales of the phugoid time histories for 2 and 5 SPS are different.

The data obtained using a sample rate of 2 SPS was totally unacceptable. For example, refering to Table VII, the value of M_u was -0.00000017 while the last step size was 0.003.

Derivatives	Z_u	X_α	X_u	X_q	M_u	X_{σ_e}
Estimate	-.003	0	-.758	-47.9	-1.7×10^{-7}	0
Standard deviation	.00006	fixed	.0542	fixed	.0002	fixed
Parameter Step Size	-.001	fixed	0.444	fixed	0.003	fixed
Eigenvalue Spread			3.54×10^8			
Likelihood Function Value			-8.4×10^3			
Time History Matches	$\sigma_\alpha = 0.0048$		$\sigma_u = 26.77$		$\sigma_q = 0.00534$	
	$\sigma_\theta = 0.053$		$\sigma_{n_z} = 2.53$			

Table VII. SCIDNT Estimates of Longitudinal Phugoid Stability Derivatives Using 2 SPS Data

Although the eigenvalue spread and likelihood function change during iteration indicate no significant program difficulties the standard deviations of the state error vector are very large. As an approximation it can be said that the phugoid maneuver is essentially a varying airspeed and pitch attitude maneuver with a constant load factor. From Table VII it can be seen that the standard deviation for airspeed was 26.77 ft/sec^{-1} and for pitch attitude was 0.053 rad, both of which were unacceptable.

The time history plots constructed using the 2 SPS data showed no real agreement between the model and the airplane. In constructing these plots both the model and airplane were excited with the same control input and the airplane time history plots superimposed on the same

scale. It is obvious that there was simply no fit of any of the state vector. It should be noted that the plot of average horizontal stabilizer position although appearing to be very rough was a result of the plot scale only and was in essense relatively smooth.

The parameter identification results using the 5 SPS data indicated it was possible to identify the phugoid mode parameters. Referring to Table VIII, it can be seen that the estimated derivatives using the 5 SPS data converged to appropriate (sign and magnitude) stability derivative values.

Derivatives	Z_u	X_α	X_u	X_q	M_u	X_{θ_e}
Estimate	-.0002	0	-.006	-45.5	-9.6×10^{-5}	0
Standard Deviation	1.2×10^{-6}	fixed	.0002	fixed	$5.\times10^{-6}$	fixed
Parameter Step Size	-8.7×10^{-6}	fixed	-.0016	fixed	-.00002	fixed
Eigenvalue Spread	1.82×10^{12}					
Likelihood Function Value	-1.49×10^{4}					
Time History Matches	$\sigma_\alpha = 0.00267$		$\sigma_u = 5.53$		$\sigma_q = 0.00343$	
	$\sigma_\theta = 0.014$		$\sigma_{n_z} = 0.92$			

Table VIII. SCIDNT Estimates of Longitudinal Phugoid Stability Derivatives using 5 SPS Data

The standard deviations of the parameter estimates were much smaller than the parameter, and the parameter step sizes

indicated that the estimates had converged to the "best" estimates obtainable with the data. It should be noted that standard deviations for u and θ were 5.53 ft sec^{-1} and 0.014 rad respectively, a significant reduction in standard deviation from those obtained with 2 SPS data

The time history plots using 5 SPS data showed relatively close agreement between the airplane and model time histories. There was, however, some model instability noted during the first 30 seconds of the time histories. It was concluded that these instabilities were due to the relatively slow sampling rate during the initial control input.

From SCIDNT the phugoid damping ratio (ζ_p) and frequency (ω_n (rad sec^{-1})) were 0.0486 and 0.06 respectfully. Available F-14 data was obtained in the auto sweep mode with SAS on while SCIDNT data was obtained in auto sweep, SAS off. It was therefore not possible to make any meaningful comparisons. However, it was noted that between 10,000 ft and 35,000 ft the phugoid period varied between 106 sec and 72 sec. The SCIDNT frequency resulted in a period of 92.53 sec which when considered in light of available NPE data appeared reasonable.

It was concluded that, within the scope of this research, the paramater identification program SCIDNT provided a reasonable estimate of the phugoid longitudinal parameters.

C. SIMULTANEOUS SHORT PERIOD AND PHUGOID PARAMETER IDENTIFICATION

1. Airplane Test Conditions

Initial trimmed test conditions for the short period

and phugoid maneuvers are presented in Table IX. Prior to the control input the airplane was trimmed for steady state "hands off" flight [5]. Since ths short period input was applied after the phugoid input, the two test conditions are different.

	Altitude (Ft HPC)	MACH	CG (% MAC)	Loading
Phugoid Input	30 326	.6217	10.86	B
Short Period Input	30 703	.5963	10.86	B

Table IX. Short Period and Phugoid Test Conditions

2. Method Of Investigation

The airplane model equations used were those shown in Appendix B. The derivatives X_{α}, X_{δ_e}, and X_q were fixed as described in the previous section.

The maneuver investigated in this section was designed specifically to provide the means of identifying the short period and phugoid parameters from one maneuver or, if you will, simultaneously. Initiation of the phugoid maneuver was accomplished in accordance with standard test techniques, [5]. Upon establishing the airplane in the phugoid maneuver, a doublet input was applied to excite the short period mode. The airplane was then allowed to fly through at least one phugoid cycle.

Identification of the short period parameters was essentially routine and straightforward. The proceedures used in estimating the parameters were those described in the previous short period section. The computer runs were made with the number of iterations and step cuts both initialized at ten. Although this short period input was superimposed on the phugoid, convergence was obtained early

in program execution. Iterations conducted under these conditions converged very quickly and executed step cuts until the allowable number was exceeded. Likelihood function change during the short period iterations was similar to that shown in Figure 2.

Based on the results of the previous section it was concluded that data recorded at 5 SPS would most likely yield reasonable phugoid parameter estimates. The short period stability derivatives obtained from this run were fixed as constants during the phugoid iterations. Computer runs were then made with the number of iterations and step cuts both initialized at ten.

Figure 6 presents the likelihood function value during iteration of the phugoid stability derivatives.

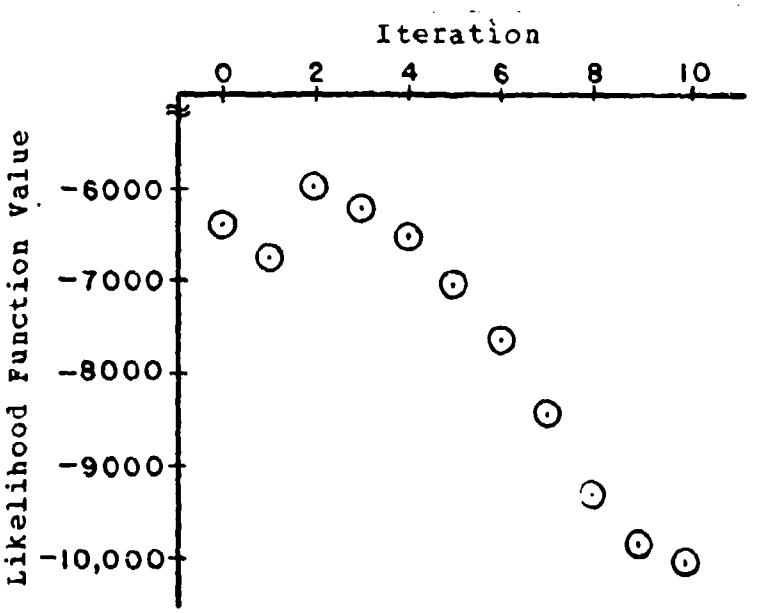

Figure 6. Likelihood Function During Iteration For Phugoid

The likelihood function change for the phugoid maneuver displayed some characteristics heretofore not encountered. The characteristics shown are typical of the results obtained with the available data. At some time during the iteration sequence the likelihood function would exhibit a jump discontinuity, in this case it occurred between the first and second iterations. Program iteration then appeared to proceed in a normal manner until the tenth iteration at which time the program terminated. From Figure 6 it was obvious that convergence had not been obtained at program termination.

In an attempt to correct the iteration instabilities the phugoid stability derivatives Z_u, X_u, and M_u were estimated simultaneously with Z_o, X_o, M_o, and Θ_o. Figure 7 presents the likelihood function during a typical iteration for seven parameters.

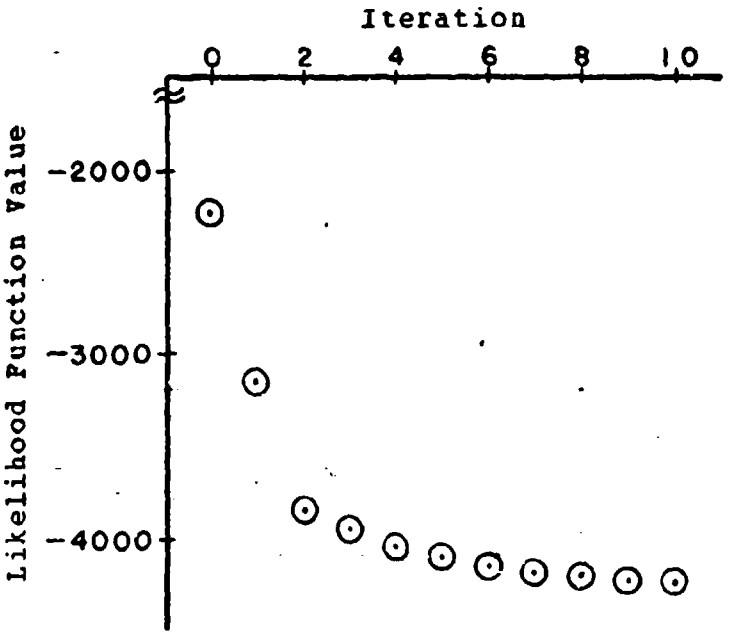

Figure 7. Likelihood Function During Iteration For Phugoid (Stability Derivatives, Z_o, X_o, M_o, and θ_o)

It can be seen that the likelihood function value converged rapidly to a steady state value with no apparent discontinuities or nonlinearaties.

3. Data Analysis

Data from a typical short period run superimposed on the phugoid are presented in Table X. A typical time history fit is presented in Appendix D, Figure 6.

Derivatives	Z_α	Z_q	M_α	M_q	Z_{δ_e}	M_{δ_e}
Estimate	-.4285	1.048	-1.54	-.665	0.19	4.464
Standard Deviation	0.0049	0.0074	0.014	0.011	0.0082	0.0312
Parameter Step Size	0.0149	0.0119	-.0166	0.0355	0.0173	-.1815
Eigenvalue Spread	1.25×10^5					
Likelihood Function Value	-4.36×10^3					
Time History Matches	$\sigma_\alpha = 0.00188$		$\sigma_u = 0.8822$		$\sigma_q = 0.0036$	
	$\sigma_\theta = 0.0048$		$\sigma_{n_z} = 1.82$			

Table X. SCIDNT Estimates of Longitudinal Short Period Stability Derivatives

The short period parameter estimates displayed characteristics similar to those observed when estimating the short period parameters from a short period input only. The time history plots showed good agreement between the model and actual airplane data. It was noted that airspeed was not constant since the short period was superimposed on the phugoid. This varying airspeed did not however, have any noticable effect on the determination of the short period parameters.

The results for the phugoid portion of the maneuver were at times in disagreement with theory. From theory it can be shown that the speed damping derivative, which acts along the negative X axis increases with speed and is therefore negative [6]. During the iteration to determine the phugoid stability derivatives it was noted that the

speed damping derivative (X_u), became positive on the seventh iteration and remained positive until program termination, Table XI.

Derivatives	Z_u	X_α	X_u	X_q	M_u	X_{δ_e}
Estimate	-.0002	0	.005	-43.85	-7.8×10^{-6}	0
Standard Deviation	1.1×10^{-6}	fixed	.0002	fixed	3.5×10^{-6}	fixed
Parameter Step Size	5.38×10^{-6}	fixed	4.8×10^{-5}	fixed	1.2×10^{-5}	fixed
Eigenvalue Spread	6.2×10^{12}					
Likelihood Function Value	-1.005×10^{4}					
Time History Matches	$\sigma_\alpha = 0.004$		$\sigma_u = 1.97$		$\sigma_q = 0.0047$	
	$\sigma_\theta = 0.031$		$\sigma_{n_z} = 1.48$			

Table XI. SCIDNT Estimates of Phugoid Stability Derivatives (Positive X_u)

The time history plots were in reasonable agreement, Appendix D Figure 7. The positive value of X_u was not however considered reasonable since this value would imply decreasing drag with increasing airspeed. The X_u term was however negative through the sixth program iteration. As mentioned previously the likelihood function during iteration showed definite signs of instability, it was

therefore suspected that the speed damping sign change was due to this program instability. The program was therefore, run again and terminated at the sixth iteration thereby producing a negative speed damping term, Table XII.

Derivatives	Z_u	X_α	X_u	X_q	M_u	X_{θ_e}
Estimate	-.00008	0	-.00032	-43.85	0.00017	0
Standard Deviation	2.6×10^{-6}	fixed	0.00047	fixed	6.7×10^{-6}	fixed
Parameter Step Size	4.0×10^{-5}	fixed	-.0059	fixed	0.000058	fixed
Eigenvalue Spread	8.53×10^{11}					
Likelihood Function Value	-7.68×10^{3}					
Time History Matches	$\sigma_\alpha = 0.0071$		$\sigma_u = 3.94$		$\sigma_q = 0.0053$	
	$\sigma_\theta = 0.0366$		$\sigma_{n_z} = 2.14$			

Table XII. SCIDNT Estimates of Phugoid Stability Derivatives (Negative X_u)

With the iterations thus restricted to six the value for X_u was maintained at a negative value. Time history plots for the negative X_u case are presented in Appendix D, Figure 8. It was noted that there was no appreciable improvement in the time history plots. In fact from Tables XI and XII it can be seen that the standard deviation of the state error

vectors was degraded for the negative X_u case. This condition in fact is however, not very startling when it is realized that the program had demonstrated instabilities and had not converged.

In an effort to reconcile these inconsistencies and lack of convergence the three phugoid parameters were estimated along with Z_o, X_o, M_o, and θ_o. This technique yielded reasonable stability derivatives and acceptable time history plots. Stability derivative data provided by the seven parameter identification are shown in Table XIII, time history plots are presented in Appendix D, Figure 9.

Derivatives	Z_u	X_α	X_u	X_q	M_u	X_{θ_e}
Estimate	-.00019	0	-.0029	-43.85	-.000141	0
Standard Deviation	1.4×10^{-6}	fixed	.00026	fixed	5.2×10^{-6}	fixed
Parameter Step Size	1.23×10^{-7}	fixed	6.3×10^{-5}	fixed	-4.02×10^{-6}	fixed
Eigenvalue Spread			3.7×10^{13}			
Likelihood Function Value			-4.23×10^{3}			
Time History Matches	$\sigma_\alpha = 0.0045$		$\sigma_u = 4.17$		$\sigma_q = 0.00523$	
	$\sigma_\theta = 0.031$		$\sigma_{n_z} = 1.86$			

Table XIII. SCIDNT Estimates of Phugoid Stability Derivatives (Parameters Estimated With Z_o, X_o, M_o, and θ_o)

The parameter standard deviations were small and within engineering tolerance. The parameter step sizes were quite small and showed further evidence of solution convergence. The standard deviation of the calculated model response with respect to the measured airplane response was acceptable. The time history plots provided further indication of parameter estimate validity.

The problems associated with the phugoid using the simultaneous technique could have been a result of program deficiencies or airplane anomalies or a combination of both. The flight conditions at which the data was obtained were areas in which the phugoid mode was lightly damped or neutrally damped. In addition the airplane wing was set to the auto sweep mode. It was felt that either of these conditions could have caused the program instabilities noted. Attempts to obtain new data were not possible due to airplane non-availability as mentioned earlier.

It was concluded that extraction of the short period stability parameters in the presence of the phugoid was easy, straight forward, and yielded results similar to those obtained from pure short period data. Estimation of the phugoid stability parameters was possible when they were estimated in conjunction with Z_o, X_o, M_o, and θ_o.

It was recommended that a new set of data be obtained at a flight condition where the phugoid is at least moderately damped and that this data be analyzed to resolve the present anomalies.

III. CONCLUSIONS

A. GENERAL

The maximum likelihood identification program SCIDNT showed great promise in obtaining the short period and phugoid stability derivatives from one maneuver, "simultaneously".

B. SPECIFIC

Within the scope of this research, the parameter identification program SCIDNT was easy and straight-forward to use in determining the short period mode.

Meaningful parameter estimates were obtainable only when started from an initial steady state condition.

Within the scope of this research, the parameter identification program SCIDNT provided a reasonable estimate of the phugoid longitudinal parameters.

Extraction of the short period stability parameters in the presence of the phugoid was easy, straight-forward, and yielded results similar to those obtained from pure short period data.

Estimation of the phugoid stability parameters was possible when they were estimated in conjunction with Z_o, X_o, M_o, and θ_o.

IV. RECOMMENDATIONS

It is recommended that a new set of data be obtained at a flight condition where the phugoid is at least moderately damped and that these data be analyzed to resolve the present anomalies.

APPENDIX A

TEST AIRCRAFT DESCRIPTION

The F-14 airplane is a supersonic, two-place, twin-engine, swing-wing, air-superiority fighter designed and manufactured by Grumman Aerospace Corporation. In addition to its primary fighter role, carrying missiles and an internal 20-millimeter gun, the airplane is designed for fleet air defense and ground attack missions. Photographs of the test airplane are shown in Figures 1 and 2. A three-view drawing is presented in Figure 3.

The forward fuselage, containing the crew and electronic equipment, projects forward from the mid fuselage and wing glove. Outboard pivots in the highly swept wing glove support the movable wing panels, which incorporate integral fuel cells and full-span leading edge slats and trailing edge flaps for supplemental lift control. In flight, the wings may be varied in sweep, area, camber, and aspect ratio by selection of any leading-edge sweep angle between 20° and 68°. Wing sweep can be automatically or manually controlled to optimize performance and thereby enhance aircraft versatility. Separate variable-geometry air inlets, offset from the fuselage in the glove, direct primary airflow to two TF30-P-412A, dual-axial-compressor, turbo-fan engines equipped with afterburners for thrust augmentation. The displaced engine nacelles extend rearward to the tail section, supporting the twin vertical tails, horizontal tails, and ventral fins. The middle and aft fuselage, which contains the main fuel cells, tapers off in depth to the rear where it accommodates the speed brake surface and arresting hook. Retractable vanes in the glove leading edges

extend to supplement lift and compensate for changes in the aircraft aerodynamic center. All control surfaces are positioned by irreversible hydraulic actuators to provide desired control effectiveness throughout the flight envelope. Stability augmentation features in the flight control system enhance flight characteristics and provide a more stable and maneuverable weapons delivery platform. The tricycle-type, forward-retracting landing gear is designed for nose gear catapult launch and carrier landings. Missiles and external stores are carried from eight hardpoint stations on the center fuselage between the nacelles and under the nacelles and wing glove; no stores are carried on the movable portion of the wing. The fuel system incorporates both inflight and single-point ground refueling capabilities.

A more complete description of the F-14A airplane is given in Ref. 8.

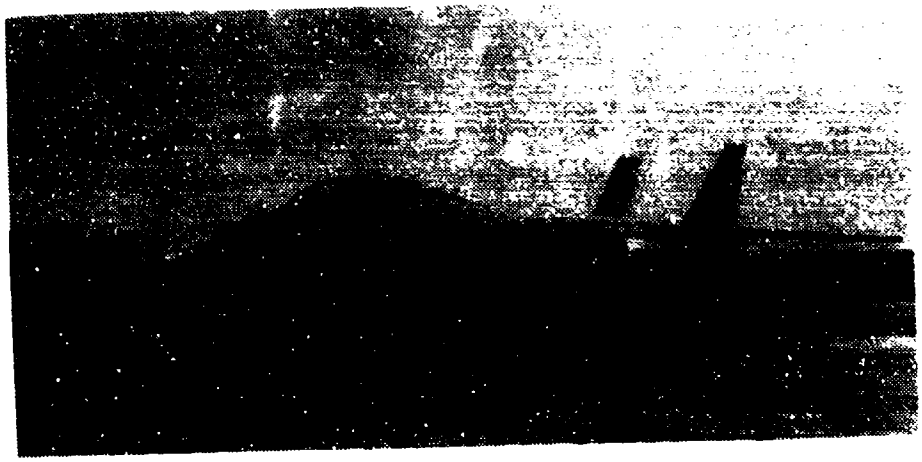

3/4 FRONT VIEW

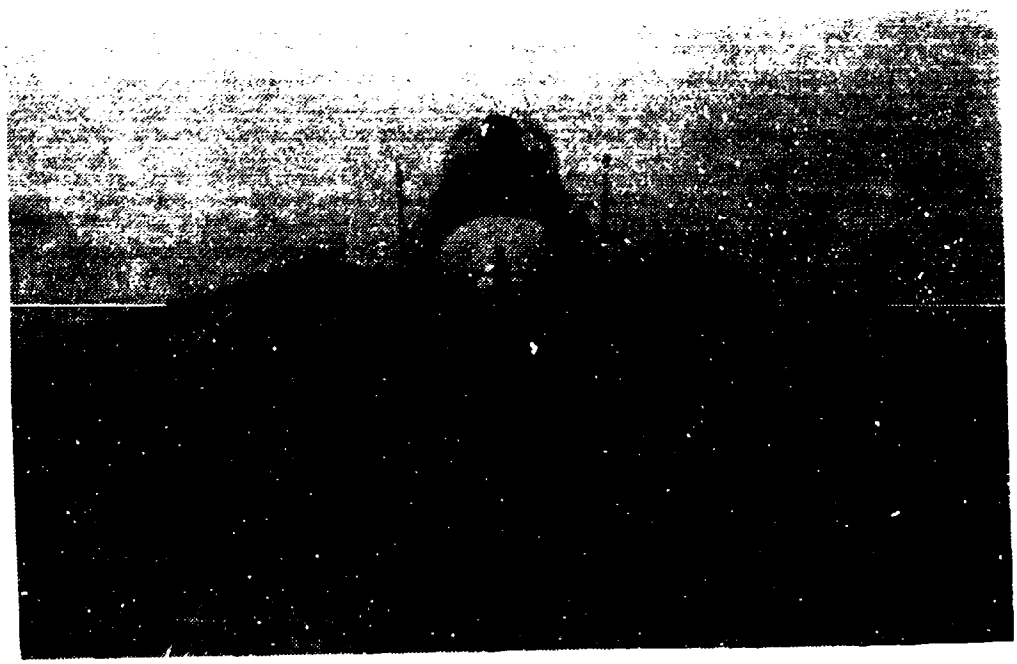

FRONT VIEW

F-14A AIRPLANE

Figure 1
APPENDIX A

SIDE VIEW

F-14A AIRPLANE

Figure 2
APPENDIX A

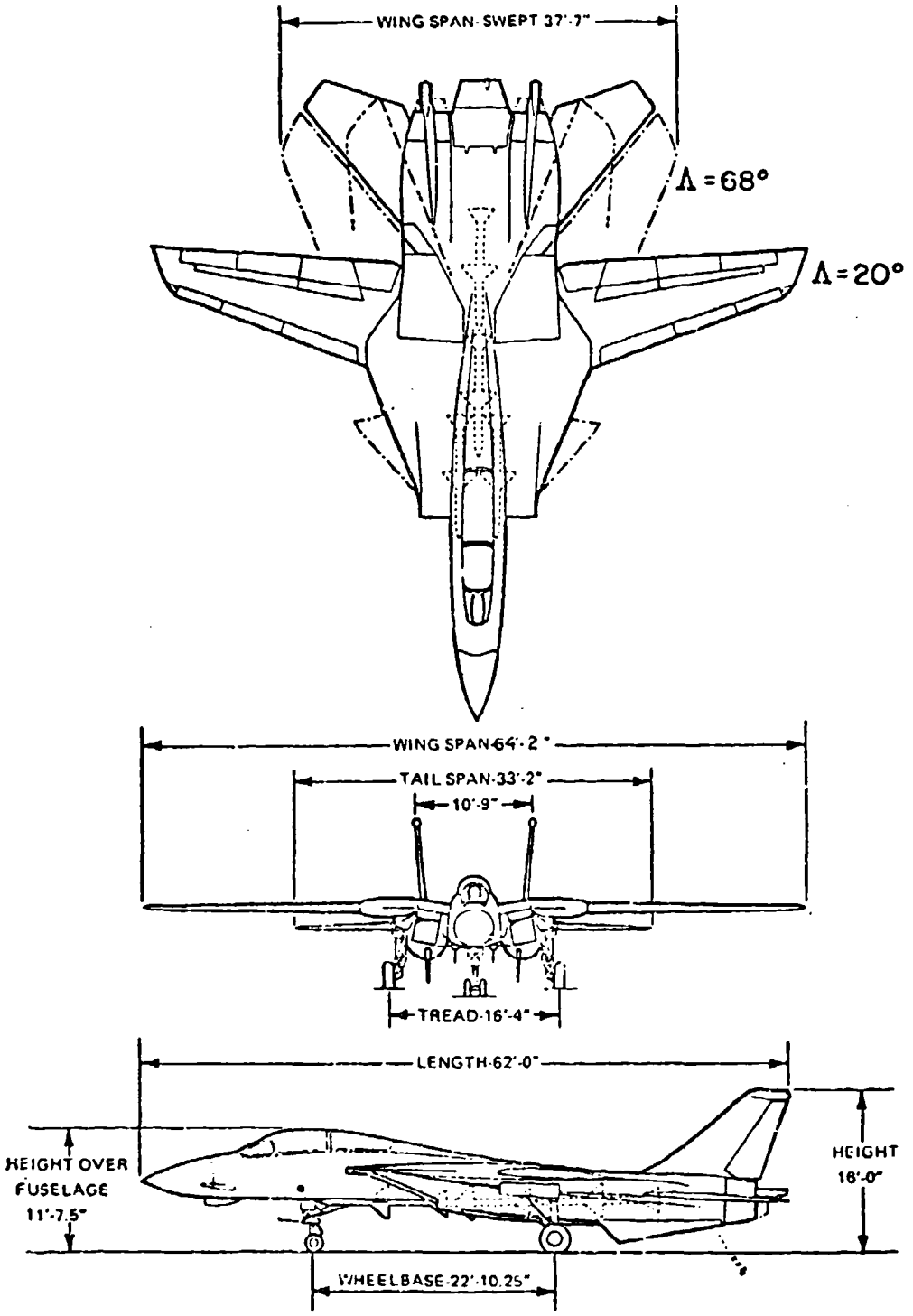

THREE VIEW DRAWING
F-14A AIRPLANE

Figure 3
APPENDIX A

APPENDIX B

DERIVATION OF THE AIRPLANE MODEL AND MEASUREMENT EQUATIONS

A detailed derivation of the complete aircraft equations of motion is shown in Ref. 6. A summary of the assumptions made during that derivation is shown below for completeness. These assumptions lead to a set of force and moment equations.

* Summary of Derivation Assumptions *

1. The airframe is a rigid body
2. The earth is fixed in space
3. The earth's atmosphere is fixed with respect to the earth
4. The mass of the airplane remained constant for the duration of any particular dynamic analysis
5. The xz plane is a plane of symmetry
6. The disturbances from the steady flight condition is small enough so that the products and squares of the changes in velocities are negligible in comparison with the changes themselves
7. The disturbance angles are small enough such that the sines of these angles may be set equal to the angles and the cosines set equal to one. Products of these angles are also approximately zero and can be neglected
8. Since the disturbances were small, the change in air density encountered by the airplane during any disturbance can be considered zero

9. During the steady flight condition, the airplane is flying with wings level and with all components of velocity zero except U_o and W_o

10. Body axis system is assumed

Dividing the force equations by the mass m and the moment equations by the appropriate moments of inertia yields terms of the form:

$$\frac{1}{m}\frac{\partial X_u}{\partial u} \qquad \text{and} \qquad \frac{1}{I_{XX}}\frac{\partial L_r}{\partial r} \qquad (B1)$$

Replacing the first term by X_u and the second term by L_r simplifies the notation. These quantities are called "dimensional stability derivatives". Using this short hand notation the equations of motion applicable to the longitudinal problem can be written as follows: (a complete set of equations is presented in Ref.5)

$$\dot{u} + W_o q + g\theta \cos\theta_o = X_u u + X_{\dot{u}}\dot{u} + X_q q + X_{\dot{q}}\dot{q}$$

$$+ X_w w + X_{\dot{w}}\dot{w} + X_{\delta_e}\delta_e + X_{\dot{\delta}_e}\dot{\delta}_e + X_{\ddot{\delta}_e}\ddot{\delta}_e$$

$$+ X_{\delta_F}\delta_F + X_{\dot{\delta}_F}\dot{\delta}_F + X_{\delta_B}\delta_B + X_{\dot{\delta}_B}\dot{\delta}_B$$

$$+ X_{\ddot{\delta}_B}\ddot{\delta}_B + \cos\xi\, T_u u + \cos\xi\, T_{\delta_{RPM}}\delta_{RPM} \qquad (B2)$$

$$\dot{w} - U_o q + g\theta \sin\theta_o = Z_u u + Z_{\dot{u}}\dot{u} + Z_q q + Z_{\dot{q}}\dot{q}$$

$$+ Z_w w + Z_{\dot{w}}\dot{w} + Z_{\delta_e}\delta_e + Z_{\dot{\delta}_e}\dot{\delta}_e + Z_{\ddot{\delta}_e}\ddot{\delta}_e$$

$$+ Z_{\delta_F}\delta_F + Z_{\dot{\delta}_F}\dot{\delta}_F + Z_{\delta_B}\delta_B + Z_{\dot{\delta}_B}\dot{\delta}_B$$

$$+ Z_{\ddot{\delta}_B}\ddot{\delta}_B - (\sin\xi)T_u u - (\sin\xi)T_{\delta_{RPM}}\delta_{RPM} \qquad (B3)$$

$$\dot{q} = M_u u + M_{\dot{u}}\dot{u} + M_q q + M_{\dot{q}}\dot{q} + M_w w + M_{\dot{w}}\dot{w} + M_{\delta_e}\delta_e$$

$$+ M_{\dot{\delta}_e}\dot{\delta}_e + M_{\ddot{\delta}_e}\ddot{\delta}_e + M_{\delta_F}\delta_F + M_{\dot{\delta}_F}\dot{\delta}_F + M_{\delta_B}\delta_B$$

$$+ M_{\dot{\delta}_B}\dot{\delta}_B + M_{\ddot{\delta}_B}\ddot{\delta}_B + \frac{z_j m}{I_{yy}}T_u u + \frac{z_j m}{I_{yy}}T_{\delta_{RPM}}\delta_{RPM} \qquad (B4)$$

In order to simplify these equations it was assumed that all disturbances were small such that the higher order terms were negligible. Also it was assumed that the flaps and speedbrakes were retracted and that thrust effects were negligible. With these further assumptions the w equation became:

$$\dot{w} - U_o q + g\theta \sin\theta_o = Z_u u + Z_q q + Z_w w + Z_{\delta_e}\delta_e \qquad (B5)$$

It was further assumed that the flow was quasisteady. Because of this all derivatives with respect to the rates of changes of velocities were omitted with the exception of those with respect to w which were retained to account for the effect on the horizontal tail of the downwash from the wing. If a wing moving through an air mass with an angle of attack α_o and a steady forward velocity U_o

is suddenly given a vertical velocity change w without changing the forward velocity, the angle of attack perturbation is as shown in Figure 1.

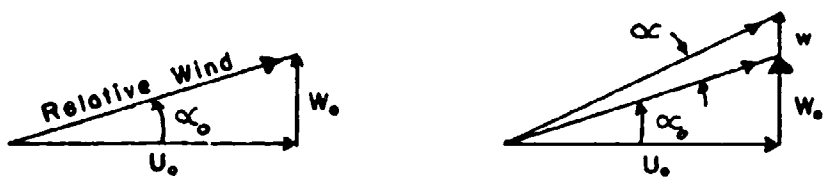

Figure 1. Angle of Attack Due to Vertical Velocity Perturbation

Thus changes in angle of attack, , are proportional to the vertical velocity perturbation w. Thus we can write,

$$\tan(\alpha_o + \alpha) = \frac{w + W_o}{\sqrt{U_o^2 + (w + W_o)^2}} \qquad (B6)$$

and by the small angle assumption

$$\alpha \cong \frac{w}{U_o} \quad \text{and} \quad \alpha_o = \frac{W_o}{U_o} \qquad (B7)$$

Taking the derivative yields,

$$\dot{w} = U_o \dot{\alpha} \qquad (B8)$$

also it can be shown that,

$$\frac{\partial Z}{\partial w} = \underset{w \to 0}{\text{Limit}} \frac{\Delta Z}{w} \qquad (B9)$$

and substituting equation B 8 yields,

$$\frac{\partial Z}{\partial w} = \underset{\alpha \longrightarrow o}{\text{Limit}} \frac{1}{U_o} \frac{\Delta Z}{\alpha} = \frac{1}{U_o} Z_\alpha \qquad (B10)$$

also if we redefine the Z dimensional derivatives such that, typically,

$$Z'_\alpha = \frac{1}{U_o} Z_\alpha \quad , \quad Z'_u = \frac{1}{U_o} Z_u \quad , \quad \hat{Z}_q = \frac{1}{u} Z_q$$

$$Z'_{\delta_e} = \frac{1}{U_o} Z_{\delta_e} \qquad (B11)$$

we can now substitute into equation B 3 which yields the equation,

$$\dot{\alpha} = Z'_\alpha \alpha + Z'_u u + Z'_q q - \frac{g}{U_o} \theta \sin \theta_o + Z'_{\delta_e} \delta_e \qquad (B12)$$

where $Z'_q = 1 + \hat{Z}_q$

A similar expression was obtained for $\dot{u}$ using the simplifying assumptions and the expressions,

$$\frac{\partial X}{\partial w} = \underset{\alpha \longrightarrow o}{\text{Limit}} \frac{1}{U_o} \frac{\Delta X}{\alpha} = \frac{1}{U_o} X_\alpha \qquad (B13)$$

and the expression for $\dot{u}$ was therefore written,

$$\dot{u} = X_\alpha \alpha + X_u u + X'_q q - g\theta \cos\theta_o + X_{\delta_e} \delta_e \qquad (B14)$$

where $X'_q = (X_q - \alpha_o U_o)$

Finally the expression for $\dot{q}$ followed directly as,

$$\dot{q} = M_\alpha \alpha + M_u u + M_q q + M_{\delta_e} \delta_e \qquad (B15)$$

The model equations for the longitudinal case, including an angle of attack due to gusts term, were written in matrix form as,

$$\dot{x} = Px + Gu + \Gamma w \qquad (B16)$$

where

state vector $x = \begin{bmatrix} \alpha \\ u \\ q \\ \theta \\ \alpha_g \end{bmatrix}$ (angle of attack perturbation); (longitudinal velocity perturbation); (pitch rate perturbation); (pitch attitude perturbation); (angle of attack due to gusts)

control vector $u = \begin{bmatrix} \delta_e \end{bmatrix}$ (horizontal elevator deflection from trim)

$$P = \begin{bmatrix} Z'_\alpha & Z'_u & Z'_q & -g/U_o \sin\theta_o & Z'_{\alpha_g} \\ X_\alpha & X_u & X'_q & -g \cos\theta_o & X_{\alpha_g} \\ M_\alpha & M_u & M_q, & 0 & M_{\alpha_g} \\ 0 & 0 & 1 & 0 & 0 \\ 0 & 0 & 0 & 0 & -\omega_c \end{bmatrix}$$

Note: Z'_q in the model is equivalent to the equation of motion term $(1 + \hat{Z}_q)$

$$g = \begin{bmatrix} Z'_{\delta_e} \\ X_{\delta_e} \\ M_{\delta_e} \\ 0 \\ 0 \end{bmatrix} \qquad \Gamma_w = \begin{bmatrix} 0 \\ 0 \\ 0 \\ 0 \\ n_6 \end{bmatrix}$$

The measurement equations written in matrix form were,

$$\dot{y} = Hx + Du + v \qquad (B17)$$

$$Hx + Du = \begin{bmatrix} K_\alpha (\alpha + \alpha_g) + \dfrac{l_\alpha K_\alpha}{U_o} q \\ u \\ q \\ \theta \\ -U_o Z_\alpha (\alpha + \alpha_g) \; Z_{\delta_e} \delta_e \end{bmatrix} \qquad v = \begin{bmatrix} n_1 \\ n_2 \\ n_3 \\ n_4 \\ n_5 \end{bmatrix}$$

Note: Selected stability derivatives are primed since they differ from the notation used in Ref. 6, however they are exactly equivalent to the derivatives used in SCIDNT.

APPENDIX C

AIRPLANE AND GROUND DATA SYSTEMS

A. AIRPLANE DATA SYSTEM

1. General

The demonstration F-14A ship number 8 BU. NO. 157987 was the test airplane utilized. A detailed description of the airplane instrumentation system is contained in Refs. 7 and 9. The airplane was modified to be compatible with the Naval Air Test Center Real-Time Telemetry Processing System (RTPS). The instrumentation systems and measurements selected for use in the test airplane were primarily designed to satisfy the Flight Test requirements for the F-14A Performance Evaluation and Demonstration. The test airplane was not entirely a production configured F-14A in that some miscellaneous cockpit components not required for flight testing were removed. The production nose radome was replaced by a fiberglass and metal radome fitted for an instrumentation noseboom assembly. Additionally, some production equipment was reworked in order to accomodate various instrumentation subassemblies.

2. Nose Boom Instrumentation

The nose boom assembly included Angle of Attack and Angle of Side Slip Vanes and a Pitot / Static Head.

3. Cockpit Instrumentation

The Forward Cockpit instrumentation was primarily pilot oriented and included; Angle of Attack and Sideslip Indicators, Airspeed, Altimeter, Machmeter, Center of Gravity Normal Acceleration and an Instrumented Control Stick. The Aft Cockpit Instrumentation included left and right engine RPM (N1), Main Fuel Flow, A/B Fuel Flow, Outside Air Temperature and the Instrumentation Master Control Console.

4. Compartment Instrumentation

The instrumentation subcomponents were mounted throughout the airplane in various available locations including, the Nose, Forward Compartments, and Equipment Compartments. The bulk of the instrumentation equipment was located in the forward equipment compartments.

5. System Description

The instrumentation system consisted of the following subsystems:

- o PCM Signal Conditioning
- o PCM
- o Timing
- o Magnetic Tape Recording
- o Telemetry
- o Power and Distribution
- o Ground Support Equipment

The system had the capacity to record on magnetic tape and to telemeter to the ground-data-reduction-complex all the PCM data for real-time analysis. The PCM Signal Conditioning Subsystem consisted of active pre-sample filter chassis and some special conditioning required for certain measurements. The pre-sample filters had cut-off frequencies

of 5, 10, 20, 40, and 80 Hz, The PCM subsystem consisted of an analog multiplexer, analog to digital converter, digital multiplexer, and the required control logic. The subsystem had the capacity of accepting up to 332 analog parameters at frequency response from dc to 40 Hz. Discrete data (On/Off signals) and a limited amount of digital data and time words were time-division multiplexed into the output data stream. The output data was presented as a succession of twelve-bit (including parity) parallel data words in NRZM format which were recorded on the digital tape. A serial output in NRZL format for entry into the "L" Band telemetry subsystem was provided. The PCM format is contained in Ref. 10. An IRIG-E Time Code Generator was installed to provide a common time correlation for magnetic tape and telemetry data. The Magnetic Tape Recording Subsystem consisted of a PCM Recorder which had the capability to record the PCM data and Time Code information. The Digital Recorder contained a sixteen track, IRIG compatible head capable of storing one hour of digital data on one inch tape at a tape speed of 30 IPS. The data was recorded in parallel using saturation recording techniques. This portion was capable of bit densities of 1000 bits per inch. The Telemetry Subsystem consisted of a signal combining unit, an "L" Band Transmitter and two blade antenna. The operating frequencies could be tuned to coinside with those in use at various test facilities. The entire Flight Test Instrumentation System was powered from the aircraft primary (generating) system. Should either the left or right engine or generator fail, the instrumentation system would continue until such time as both generators failed. The distribution system consisted of a 28V dc transformer/rectifier (T/R), and a power/control distribution box, which provided electrical system protection and isolation from the aircraft power systems through individual circuit breakers. The equipment required to perform checks on the installed instrumentation systems was configured in mobile test carts. These carts

required only 60 cycle power for operation and provided the operator with a tool for conducting pre-flight and post flight tests on the tape recording system.

B. GROUND DATA SYSTEM

The Naval Air Test Center, Patuxent River, Maryland, employs a Real-Time Telemetry Processing System (RTPS) as universal support for testing on several types of aircraft and weapons systems, Ref. 10. The computer system, designed by Xerox, consists of a Sigma 9 general purpose computer as the central processor supported by three Sigma 3 computers performing the data input and output processing. RTPS provides the capability to process two complete and independent tests (data "streams") simultaneously from either tape or telemetry sources. These "streams" can support totally unrelated and asynchronous test flights or can support setup for one flight while processing another flight.

Each Data Channel accepts up to 512 channels of PCM data and 32 parameters of FM data. This data is processed (individually or mixed) by a Sigma 3 and preprocessing Programmed Algorithm Unit (PAU). Up to 50,000 values of Engineering Units (EU) data per second can be fed to the Sigma 9 while simultaneously being stored on digital tapes for later playback. Two large screen interactive graphic display stations, that provide real-time "hands on" data analysis and presentation, are controlled by the Sigma 3 Display Processor. Batch jobs can be processed when the real-time and non real-time operational modes are not utilizing the resources of the system to 100 percent. The batch job is defered if additional demands are made by either non real-time or real-time tasks during batch job processing.

The specific flight test data utilized by the parameter

identificatiom program were, V_T, ALPHA FRL, pitch rate, pitch attitude, NZ NET, and average horizontal stabilizer position. The raw data (digital) was used to generate an EU tape for input to the parameter identification program. in generating the EU tape corrections were made to the measured values as required in accordance with Ref 11. For example corrections to angle of attack included nose boom bending moments, fuselage bending moments and pitch.

APPENDIX D

TIME HISTORY FITS

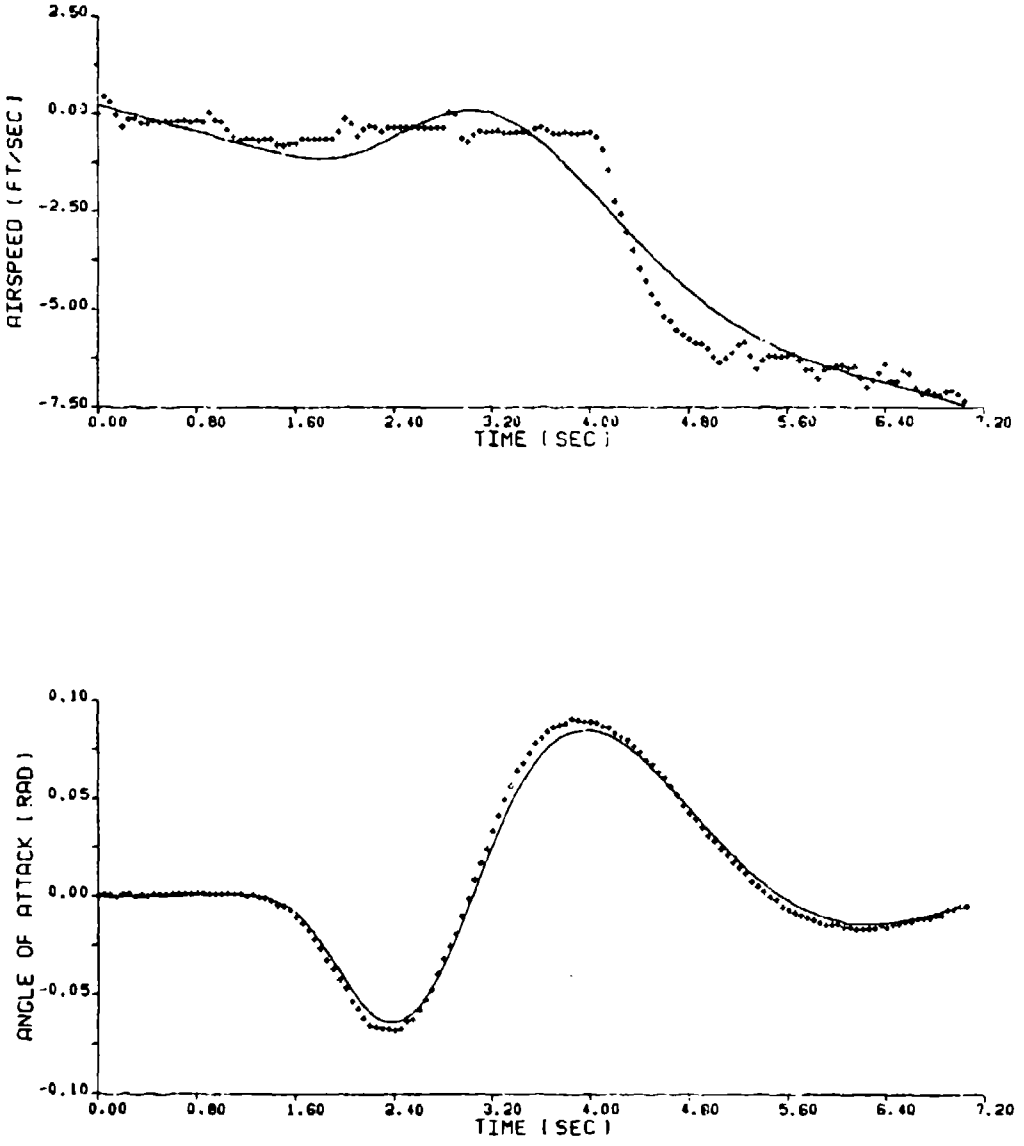

Short Period Time History Using Doublet Input

Figure 1
APPENDIX D
Page 1 of 3

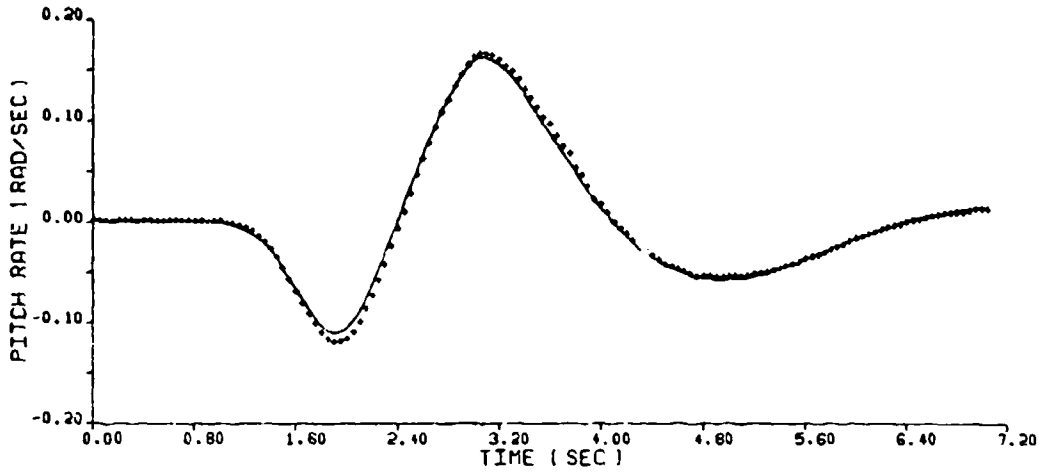

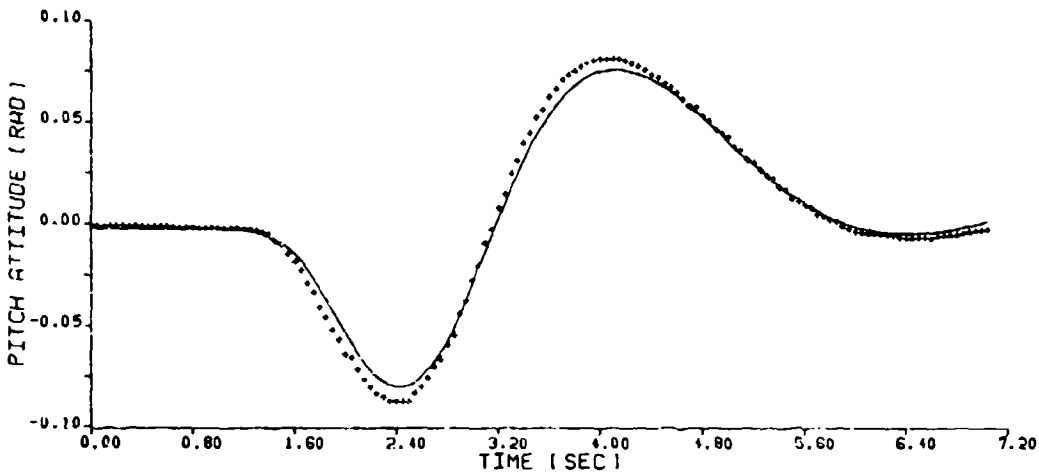

Short Period Time History Using Doublet Input

Figure 1
APPENDIX D
Page 2 of 3

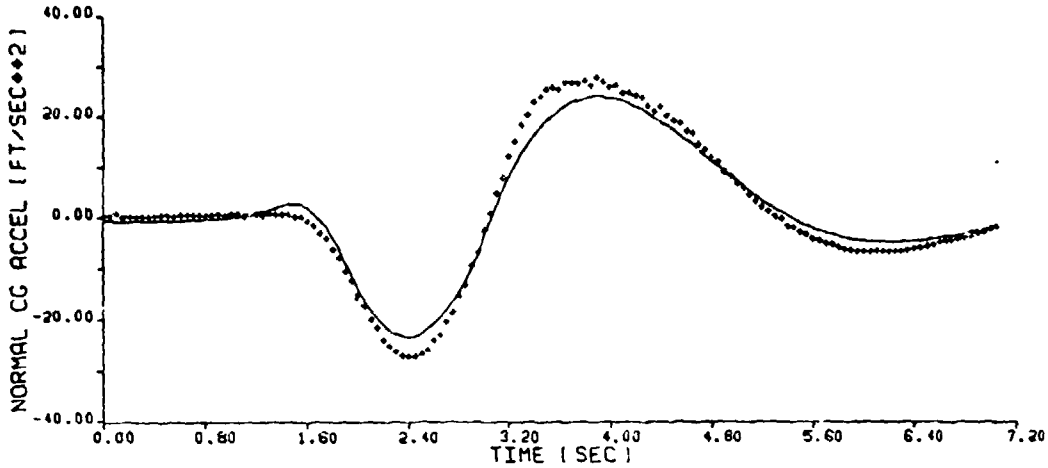

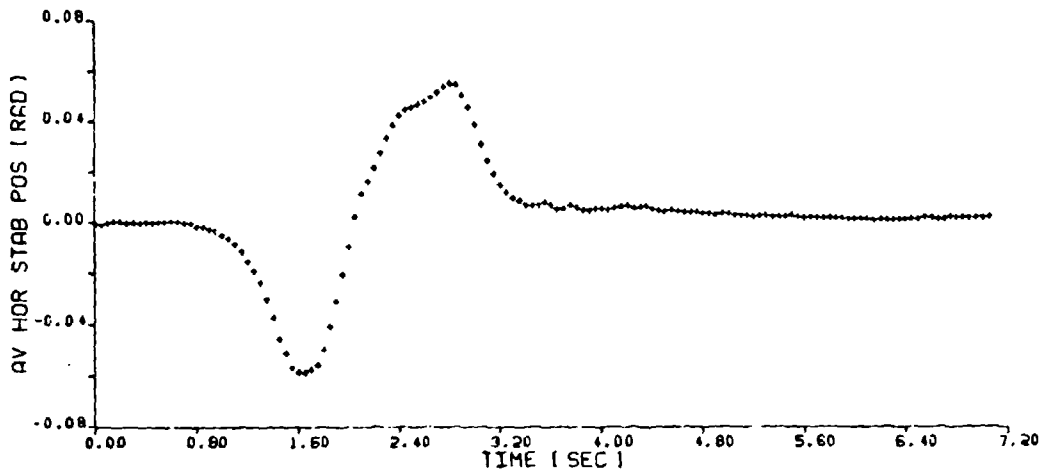

Short Period Time History Using Doublet Input

Figure 1
APPENDIX D
Page 3 of 3

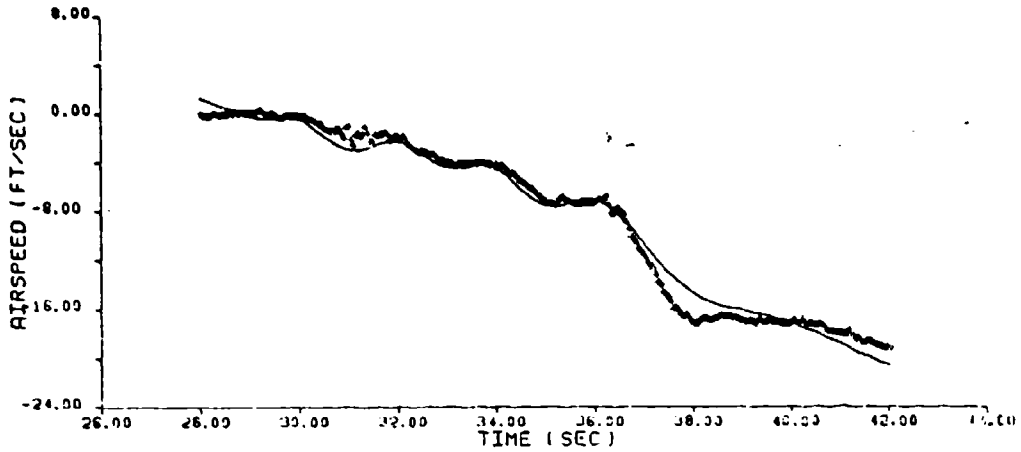

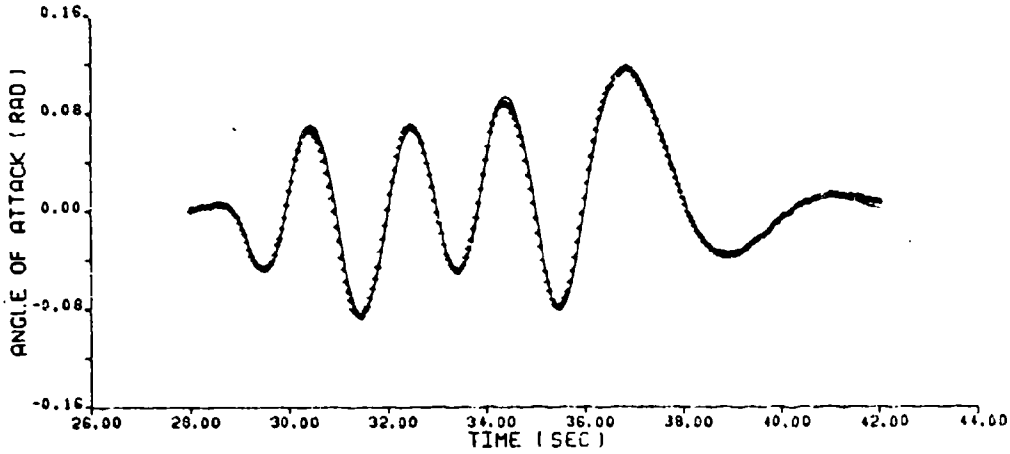

Short Period Time History Using Sinusoidal Input

Figure 2
APPENDIX D
Page 1 of 3

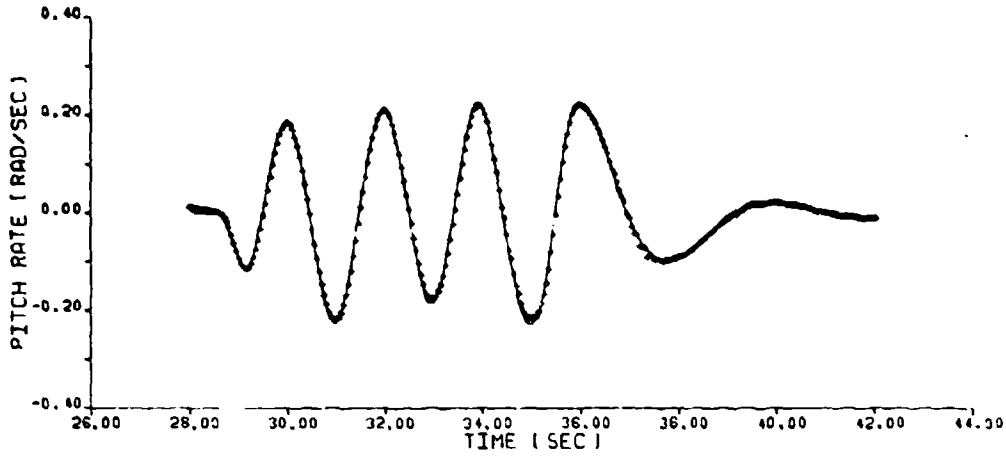

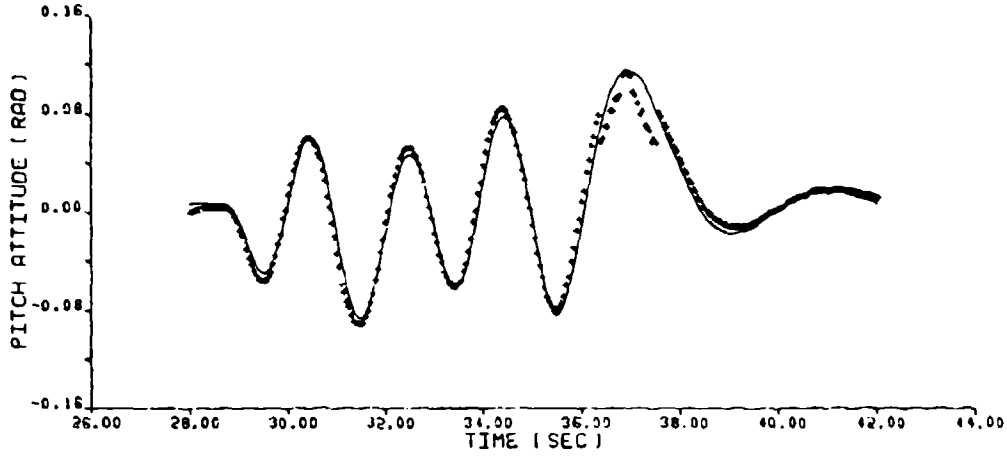

Short Period Time History Using Sinusoidal Input

Figure 2
APPENDIX D
Page 2 of 3

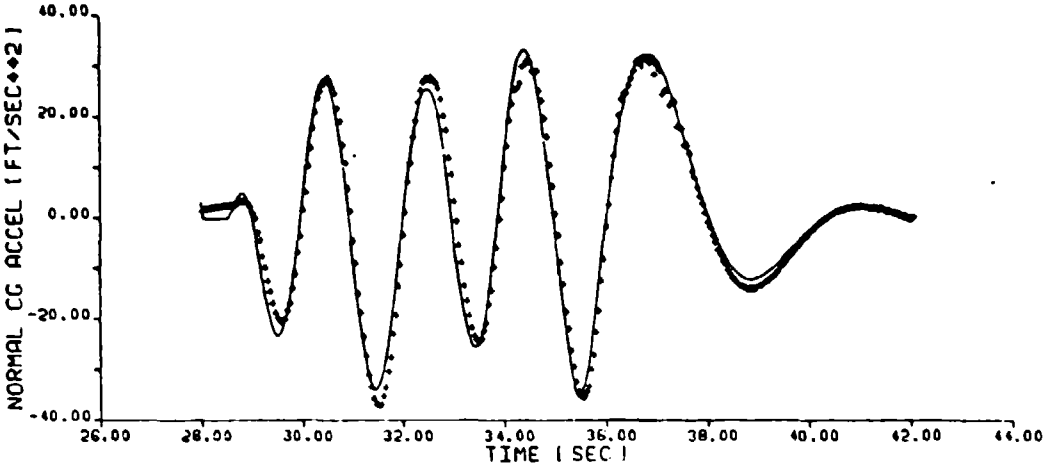

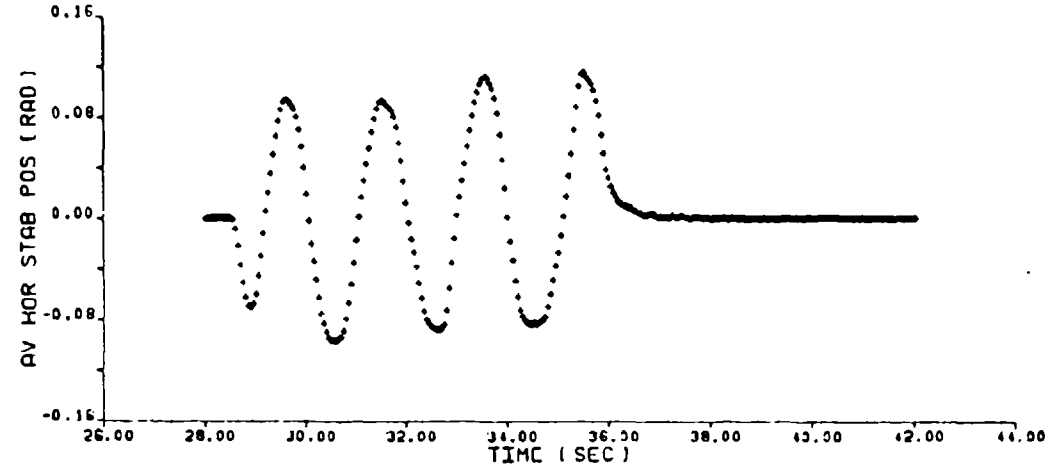

Short Period Time History Using Sinusoidal Input

Figure 2
APPENDIX D
Page 3 of 3

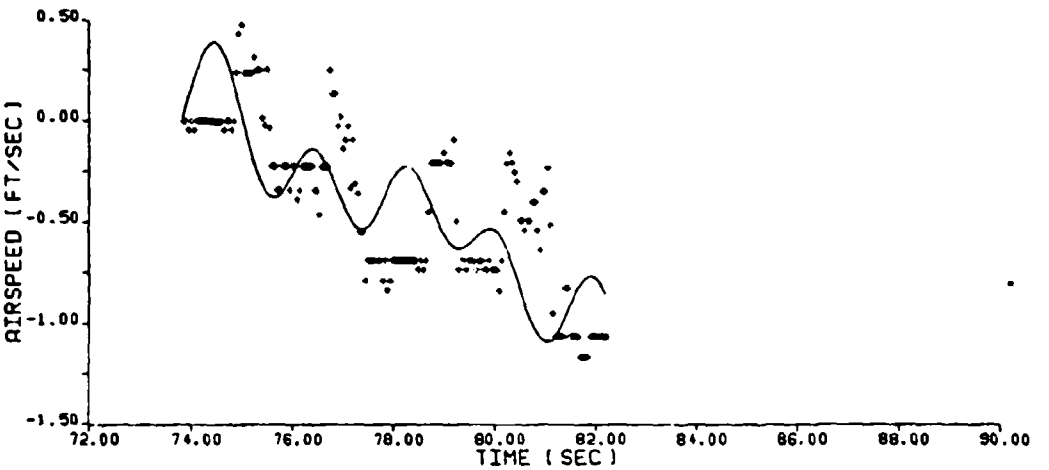

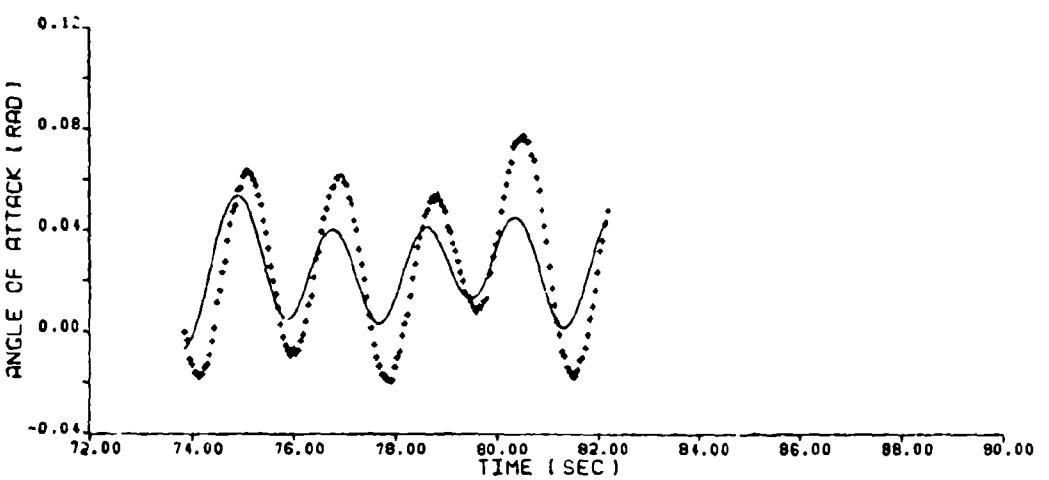

Short Period Time History With Non-zero Initial Conditions

Figure 3
APPENDIX D
Page 1 of 3

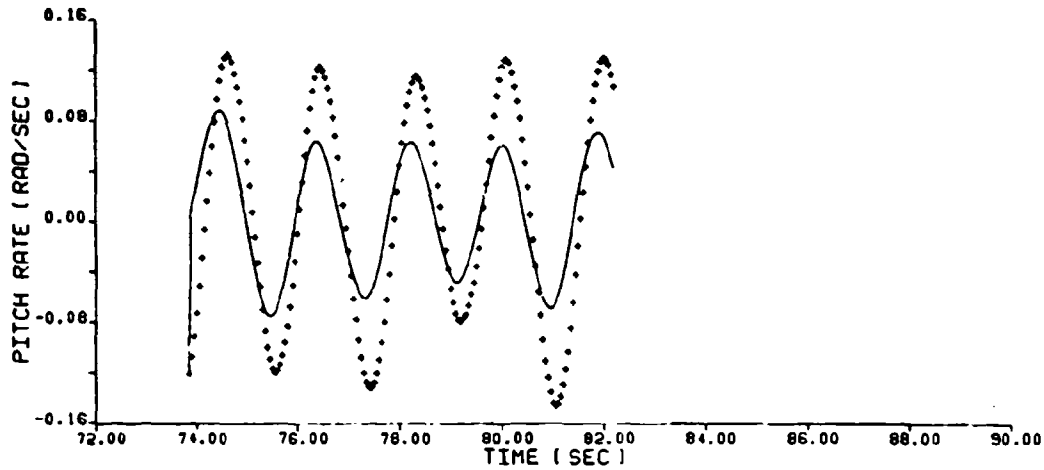

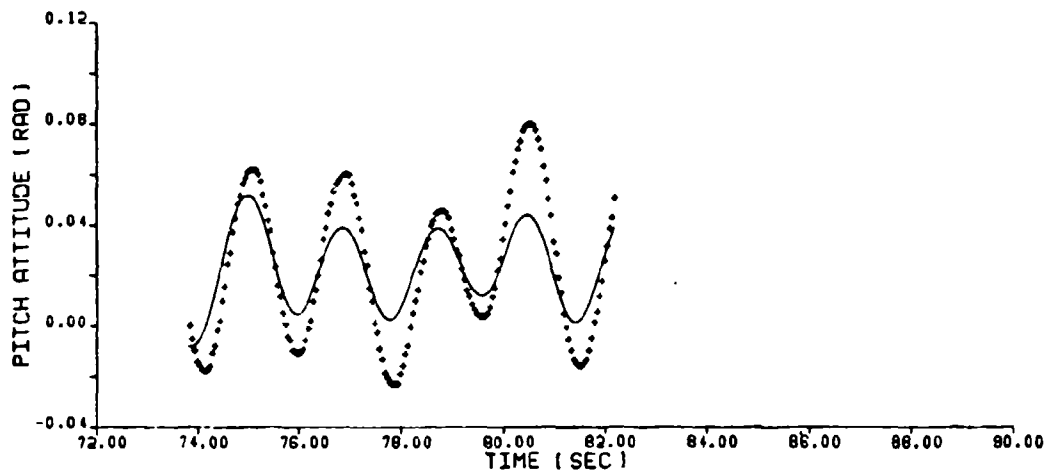

Short Period Time History With Non-zero Initial Conditions

Figure 3
APPENDIX D
Page 2 of 3

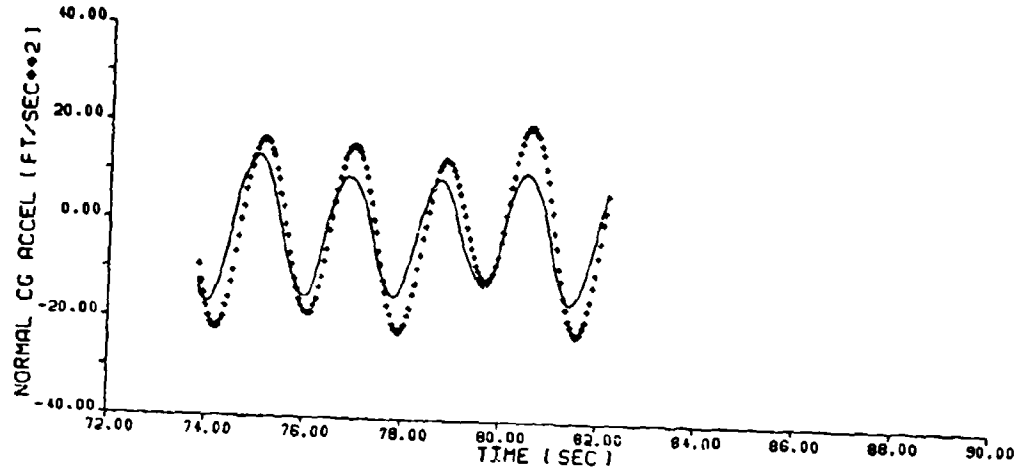

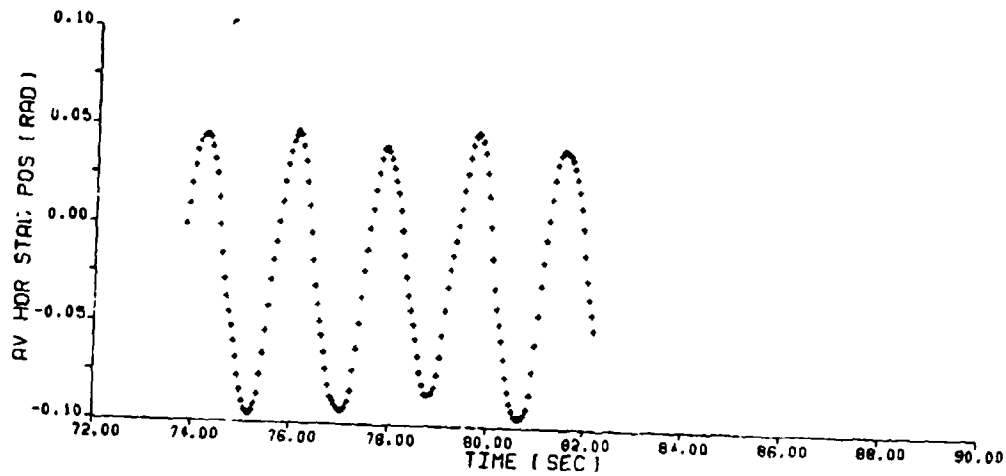

Short Period Time History With Non-zero Initial Conditions

Figure 3
APPENDIX D
Page 3 of 3

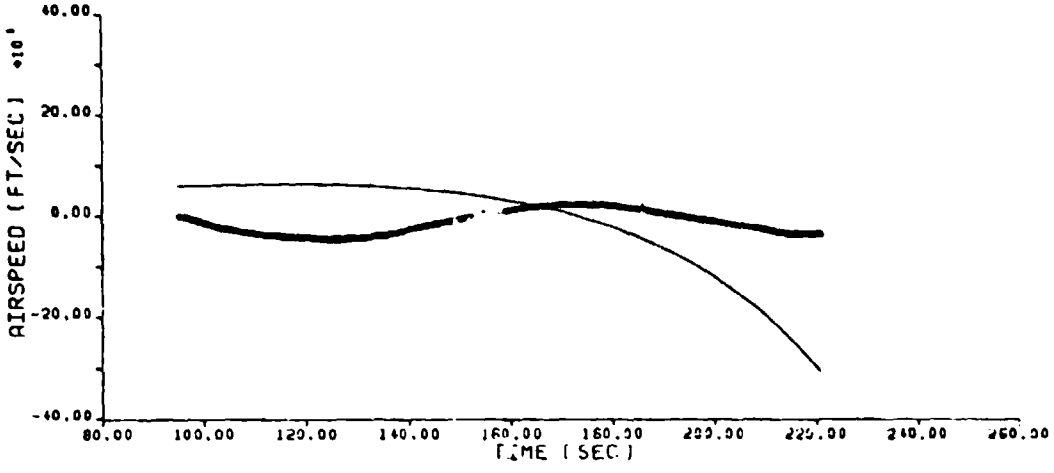

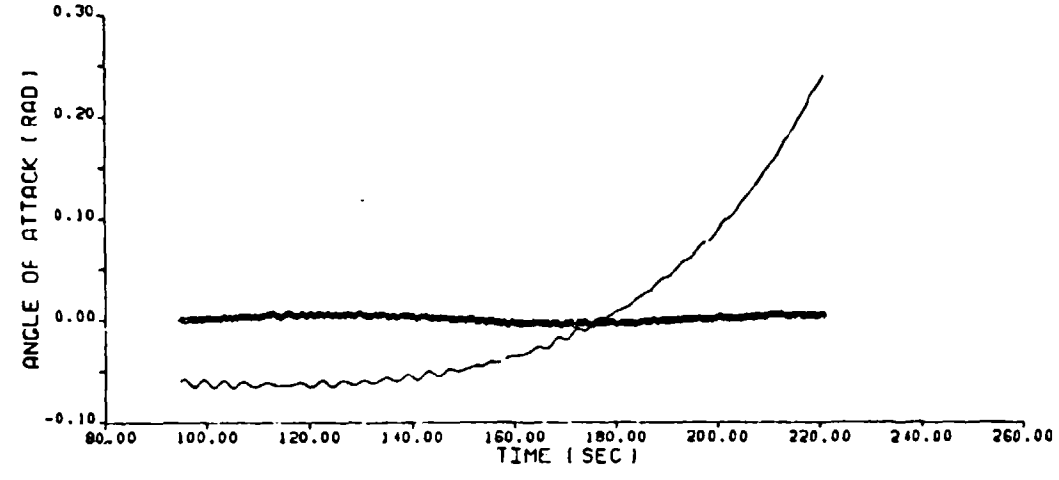

Phugoid Time History Using 2 SPS Data

Figure 4
APPENDIX D
Page 1 of 3

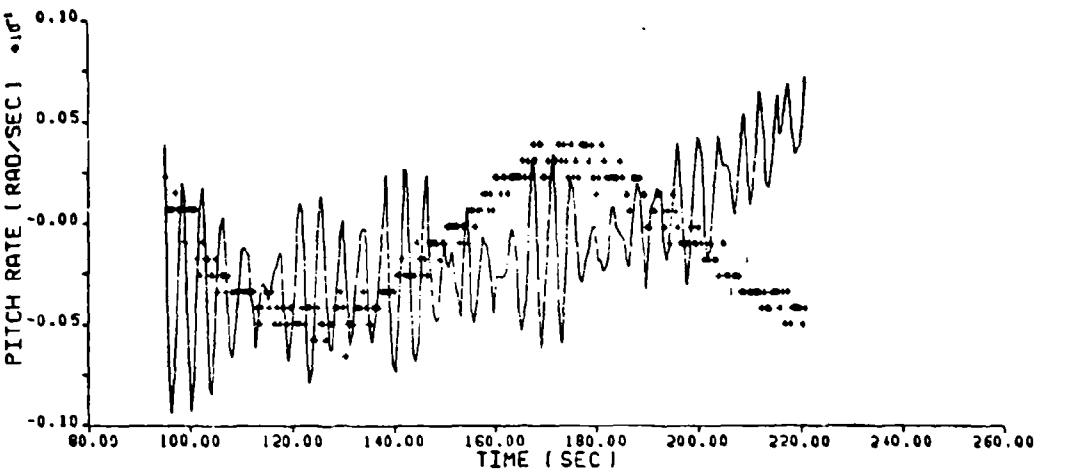

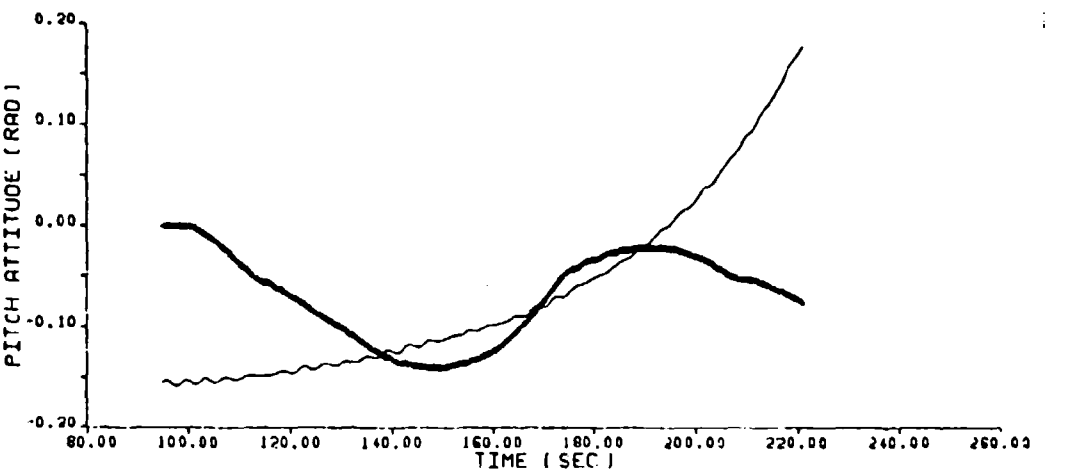

Phugoid Time History Using 2 SPS Data

Figure 4
APPENDIX D
Page 2 of 3

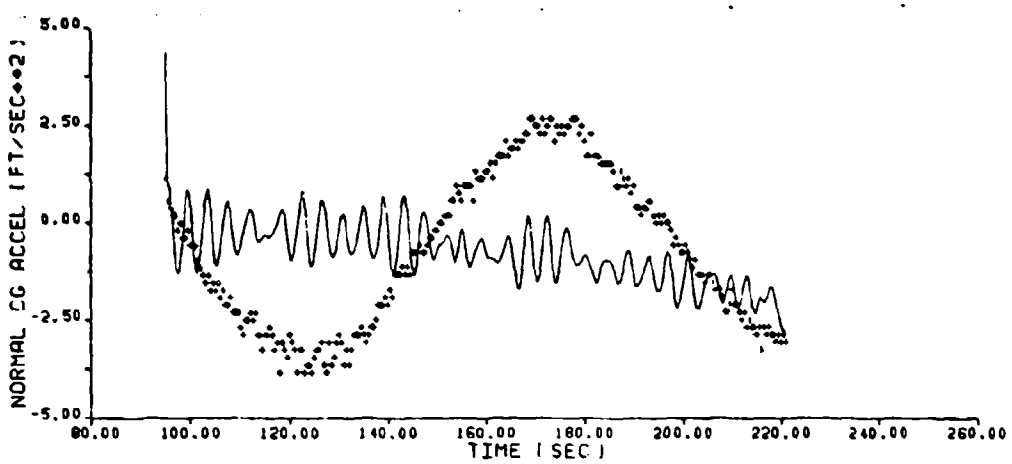

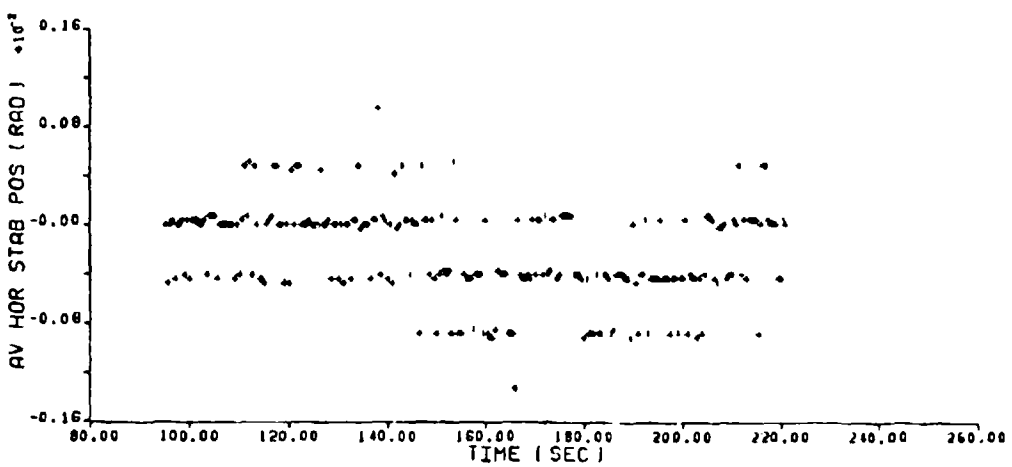

Phugoid Time History Using 2 SPS Data

Figure 4
APPENDIX D
Page 3 of 3

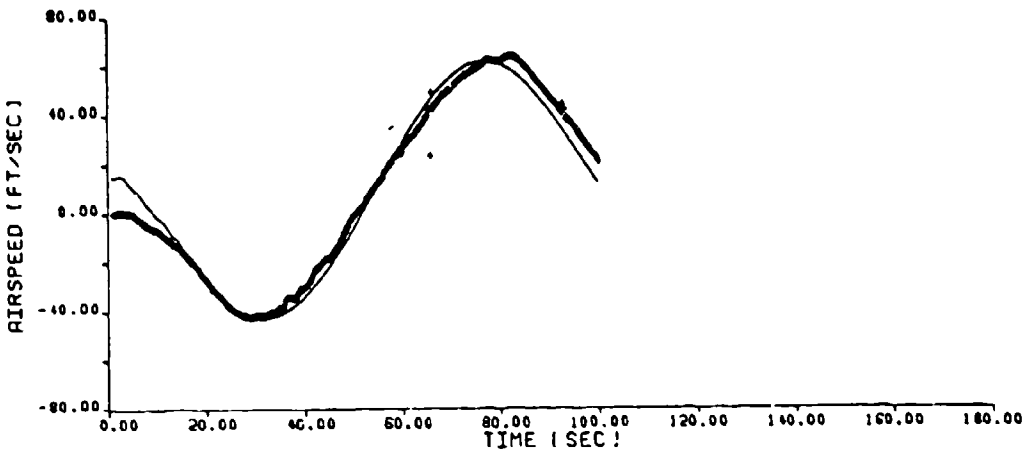

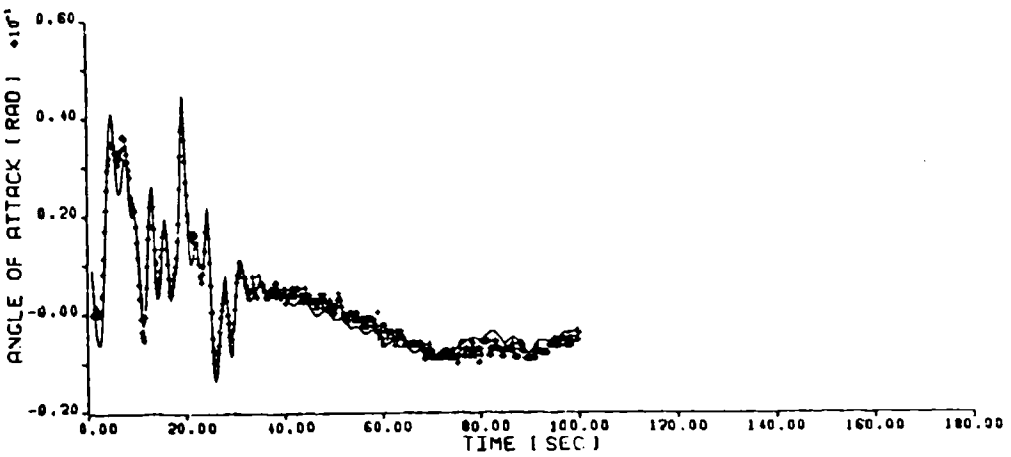

Phugoid Time History Using 5 SPS Data

Figure 5
APPENDIX D
Page 1 of 3

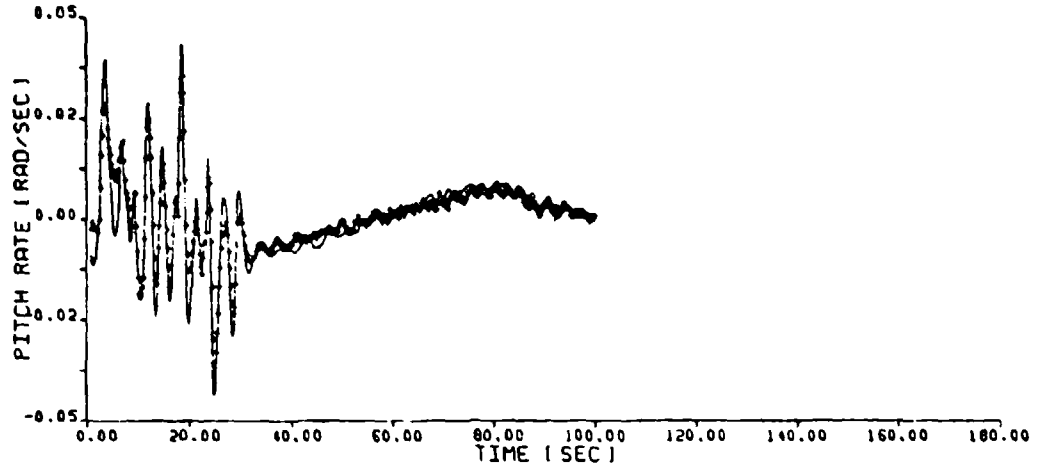

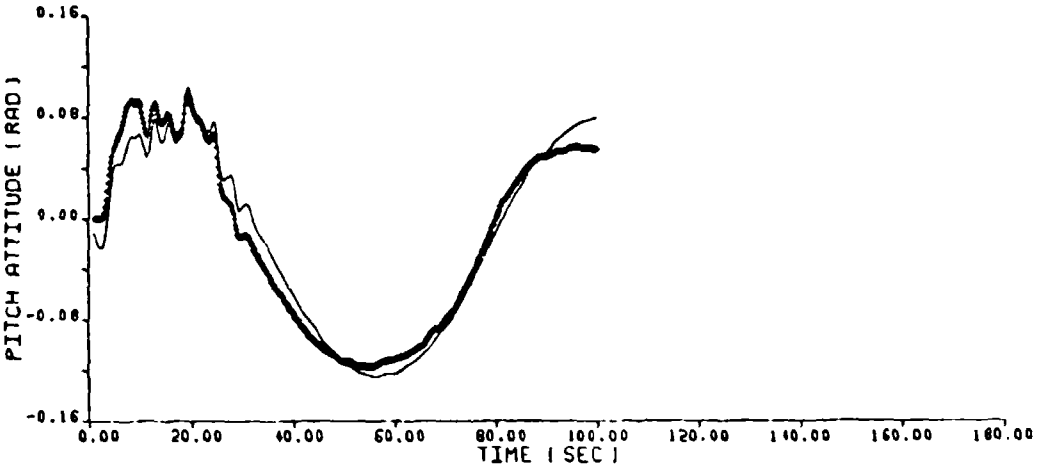

Phugoid Time History Using 5 SPS Data

Figure 5
APPENDIX D
Page 2 of 3

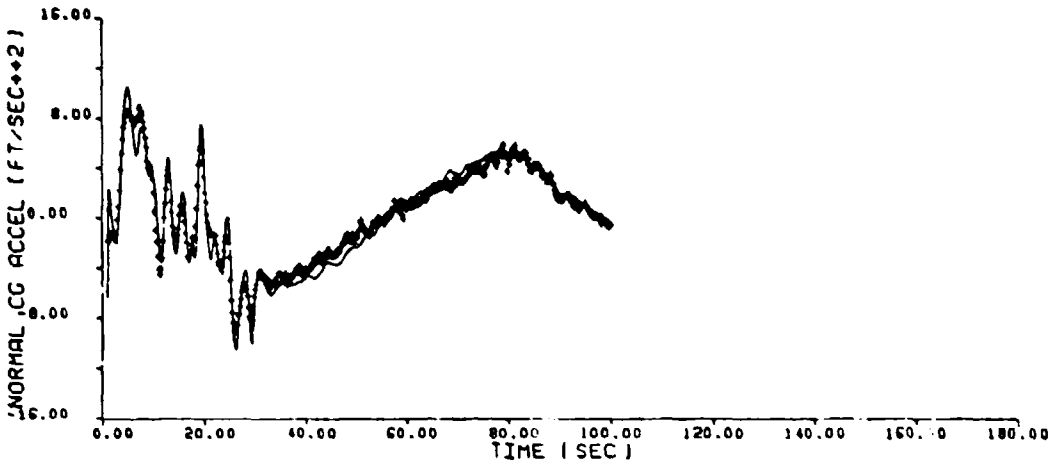

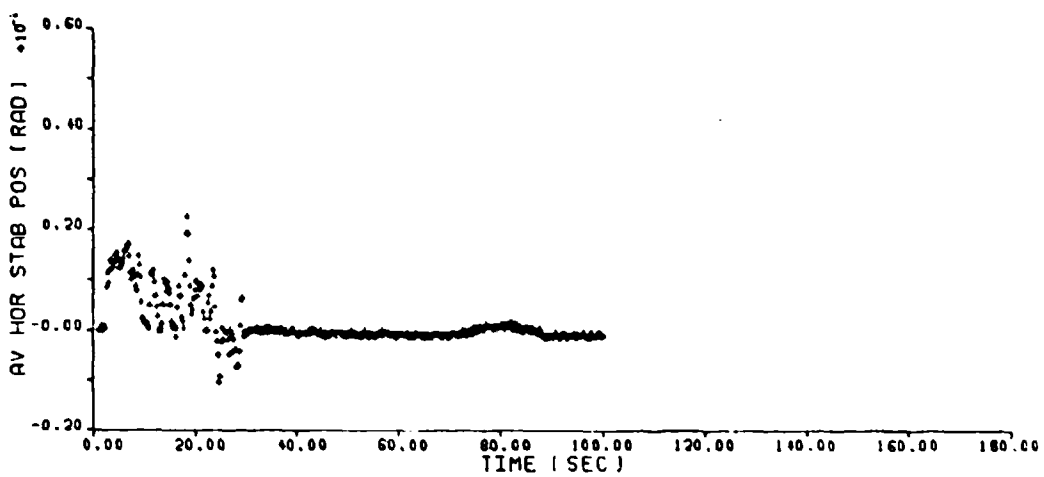

Phugoid Time History Using 5 SPS Data

Figure 5
APPENDIX D
Page 3 of 3

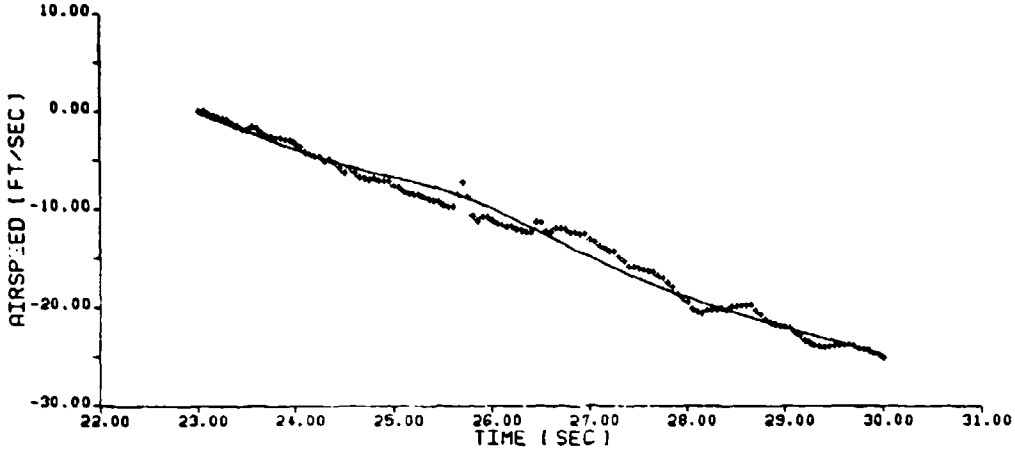

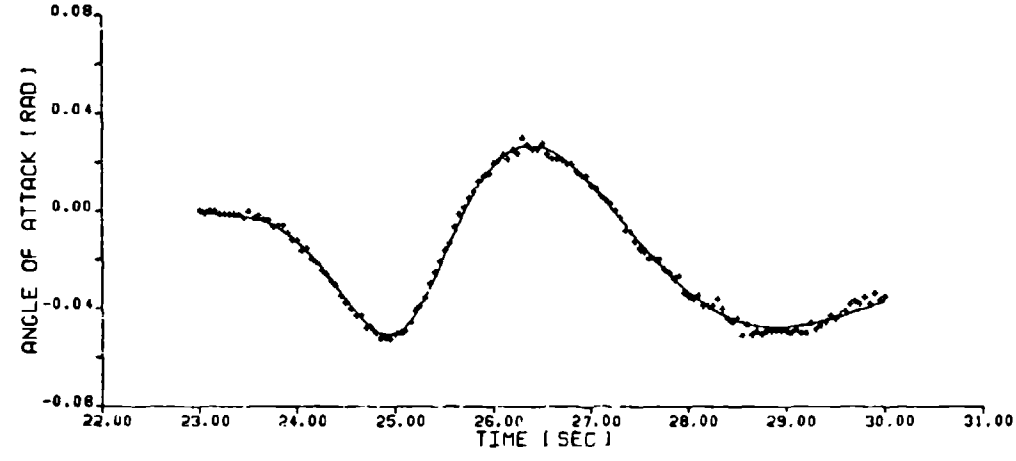

Short Period Time History Superimposed On Phugiod

Figure 6
APPENDIX D
Page 1 of 3

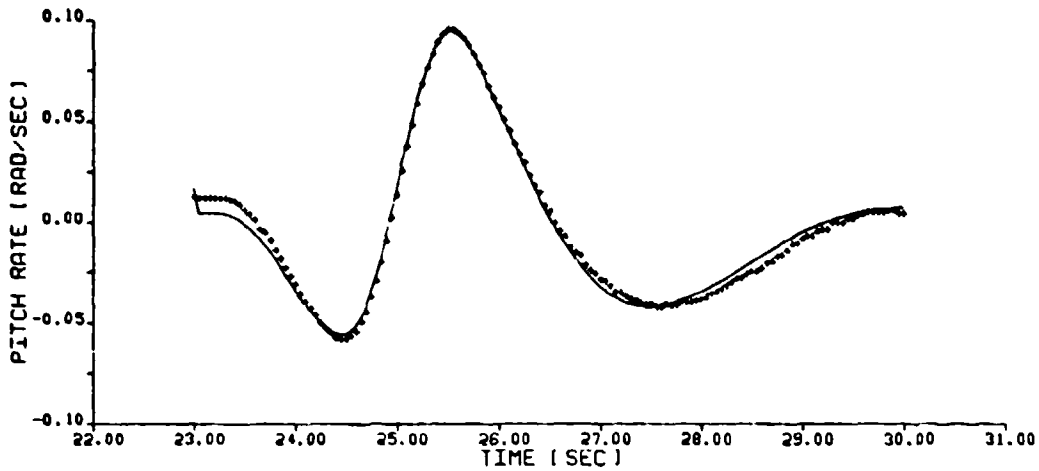

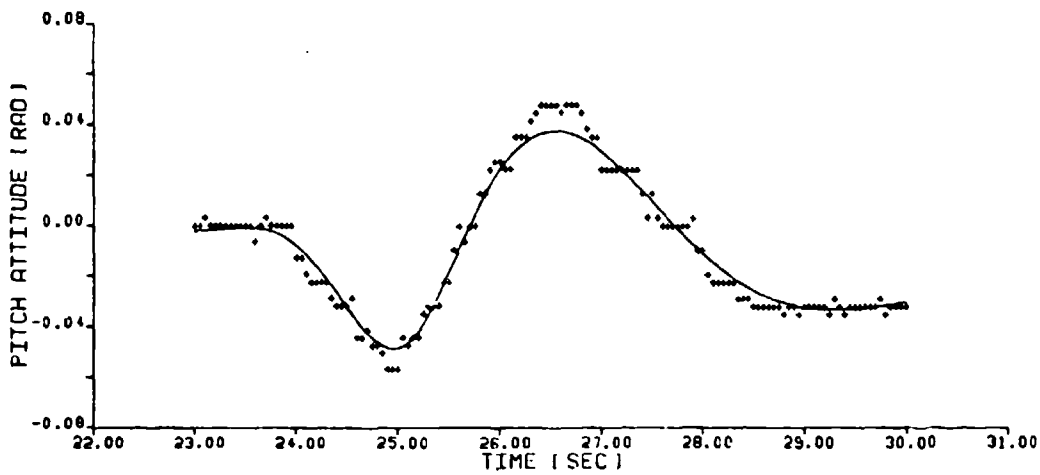

Short Period Time History Superimposed On Phugiod

Figure 6
APPENDIX D
Page 2 of 3

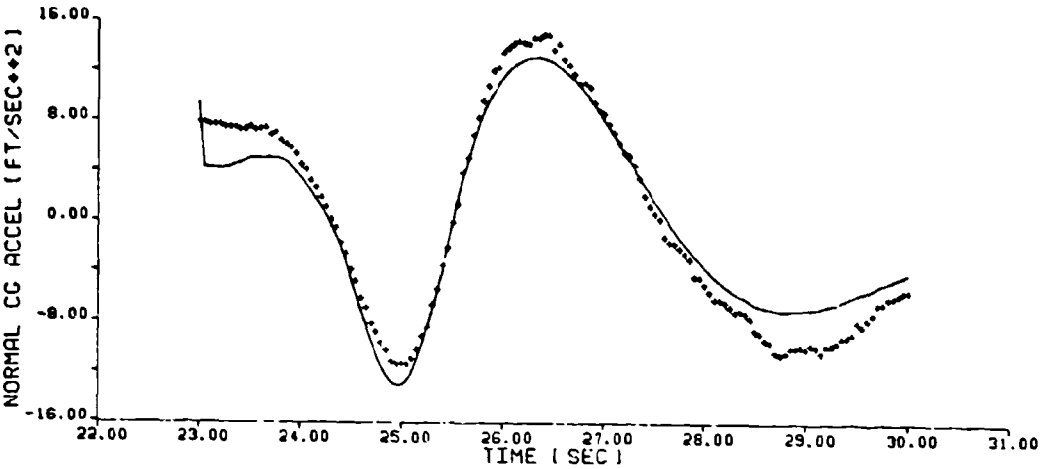

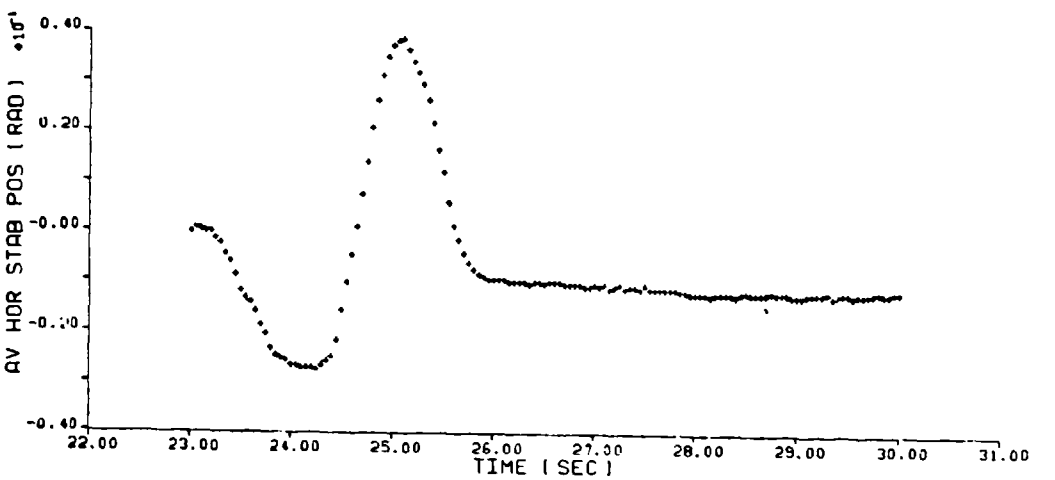

Short Period Time History Superimposed On Phugiod

Figure 6
APPENDIX D
Page 3 of 3

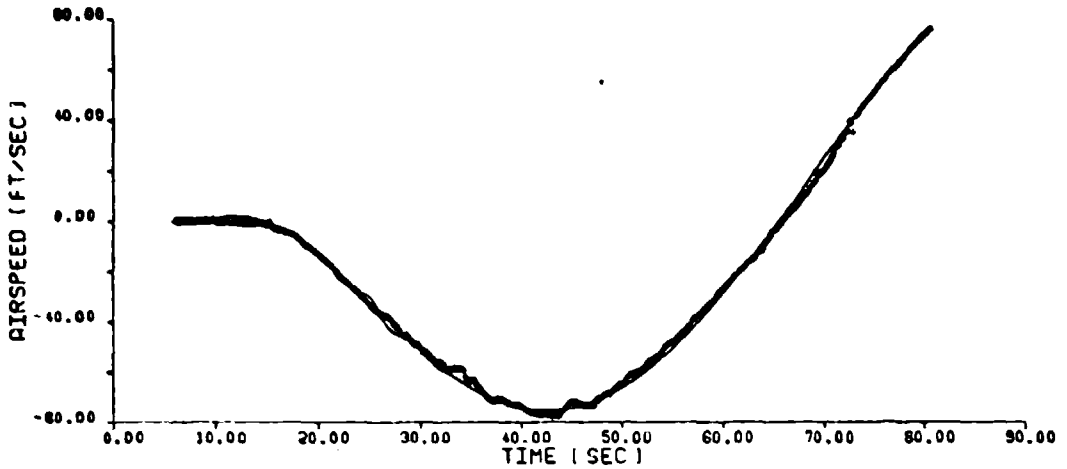

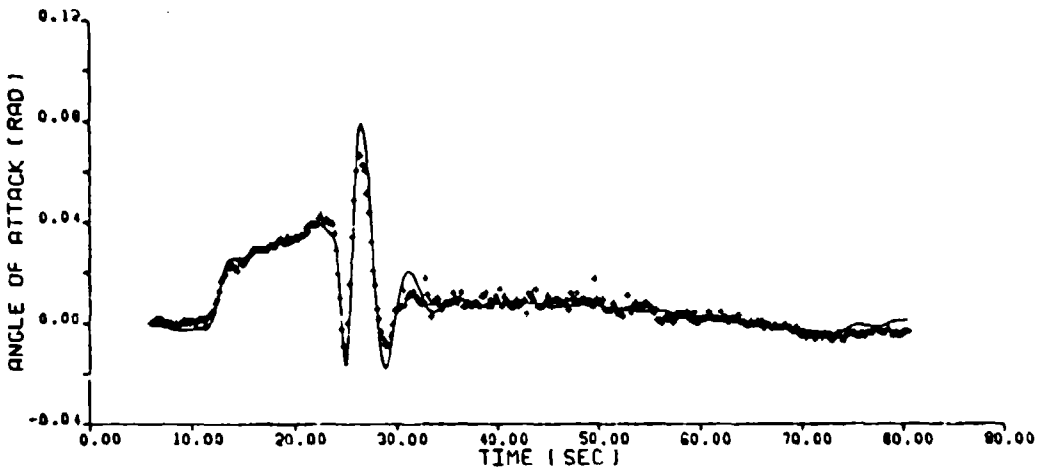

Phugoid Time History With
(Positive X_u)

Figure 7
APPENDIX D
Page 1 of 3

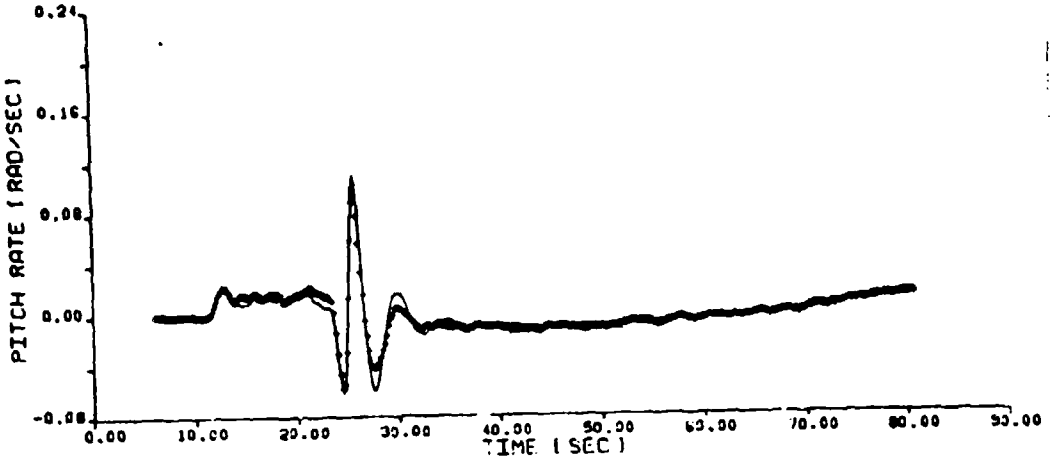

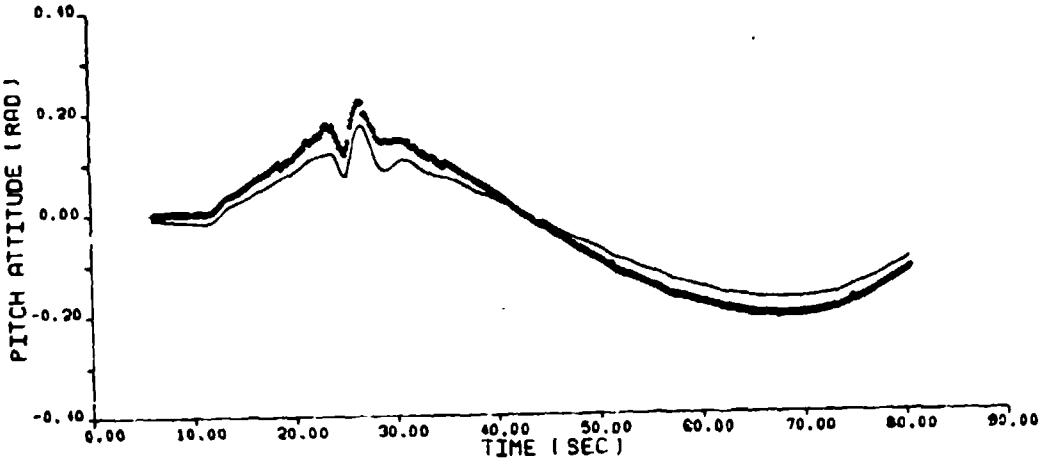

Phugoid Time History With
(Positive X_u)

Figure 7
APPENDIX D
Page 2 of 3

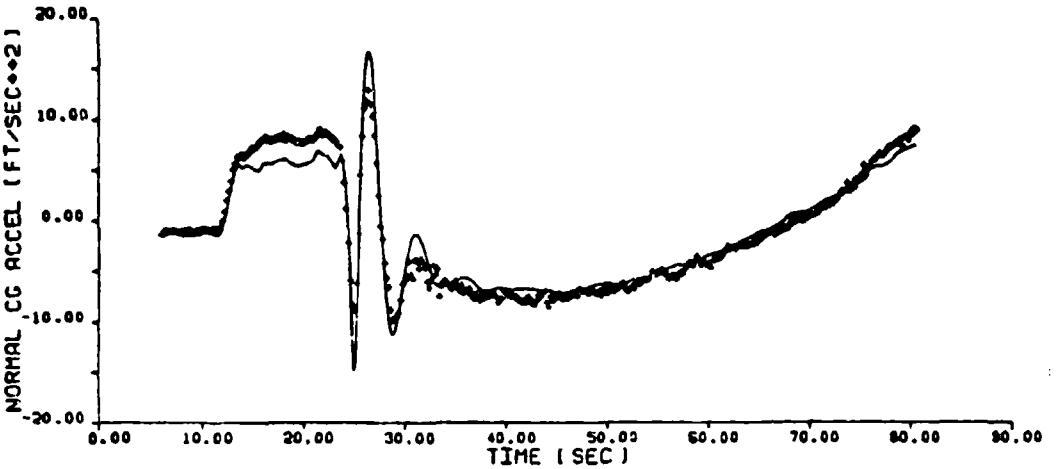

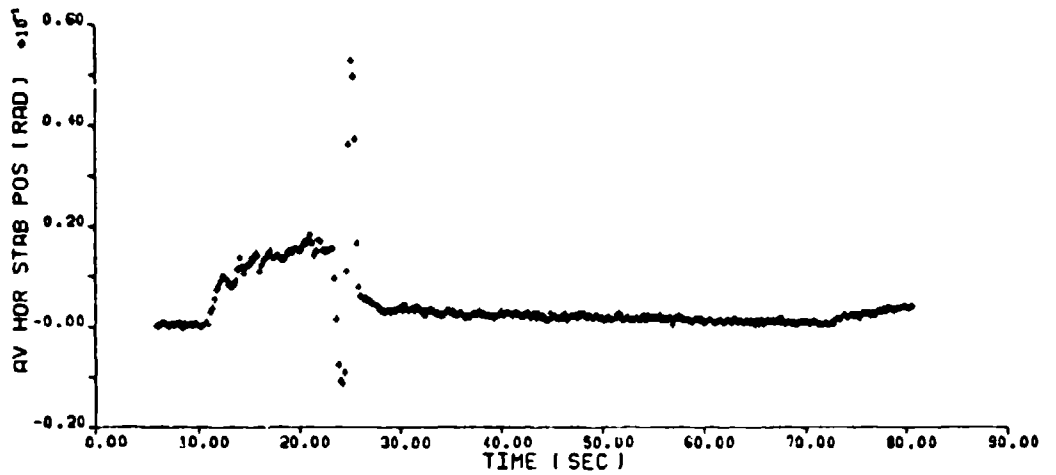

Phugoid Time History With
(Positive X_u)

Figure 7
APPENDIX D
Page 3 of 3

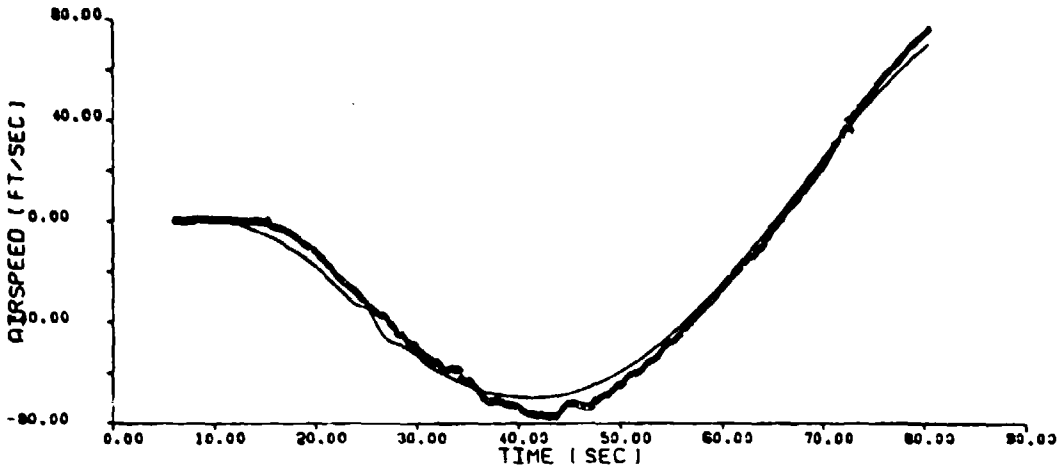

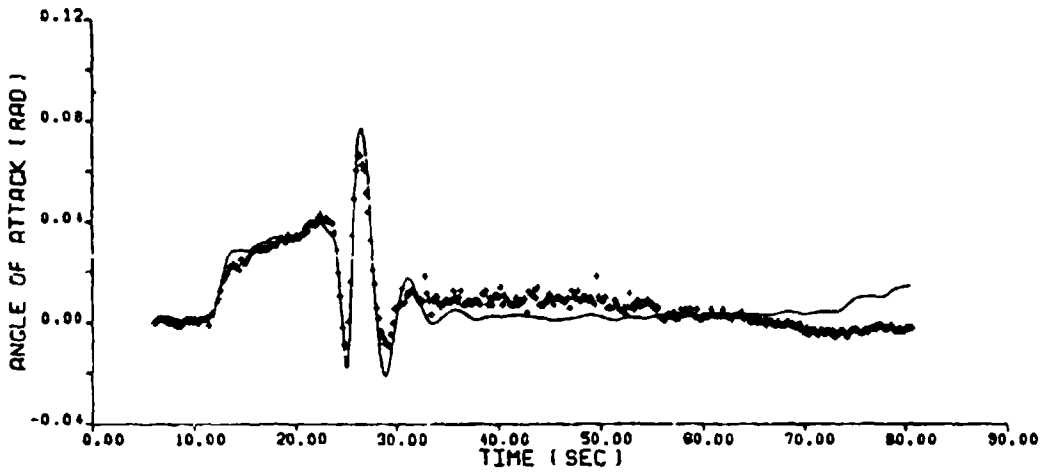

Phugoid Time History With
(Negative X_u)

Figure 8
APPENDIX D
Page 1 of 3

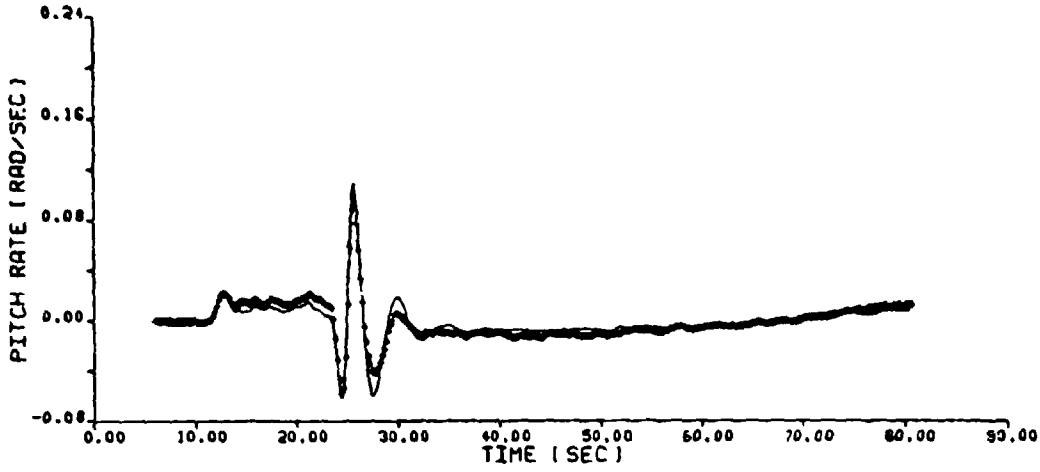

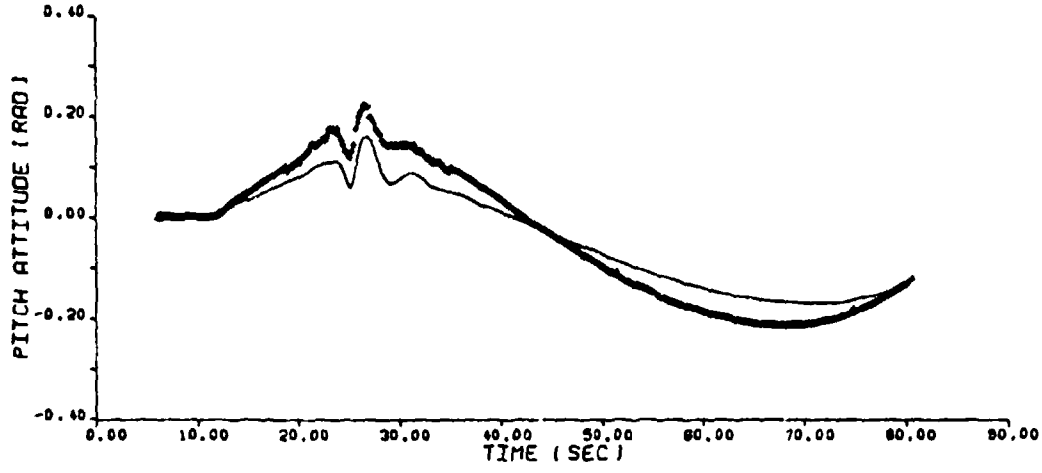

Phugoid Time History With
(Negative X_u)

Figure 8
APPENDIX D
Page 2 of 3

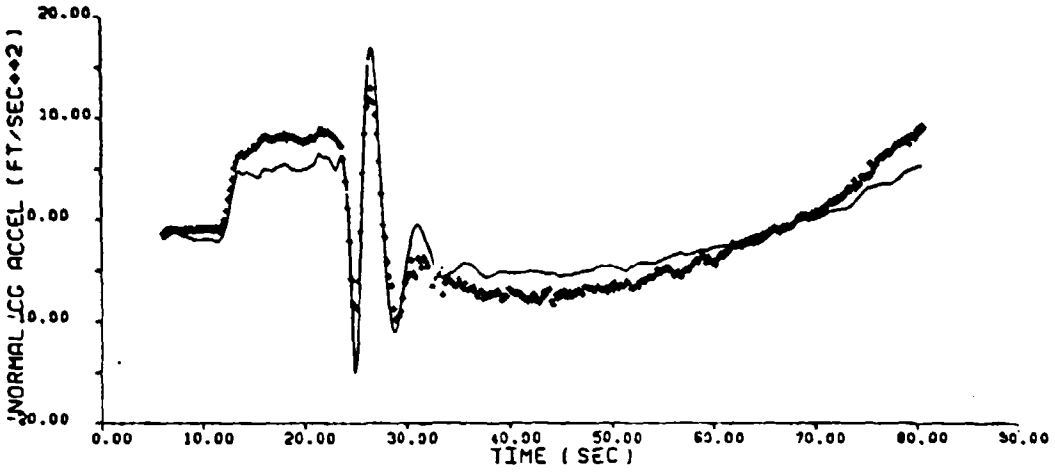

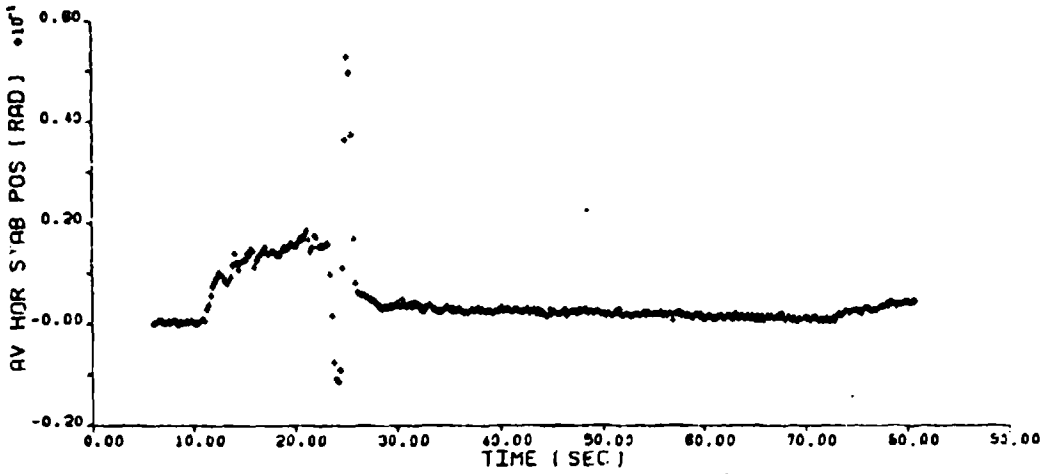

Phugoid Time History With
(Negative X_u)

Figure 8
APPENDIX D
Page 3 of 3

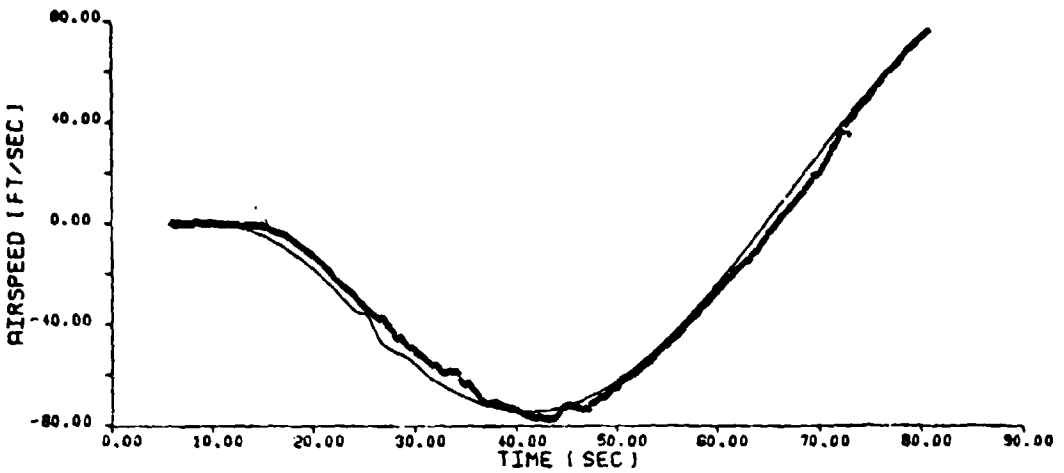

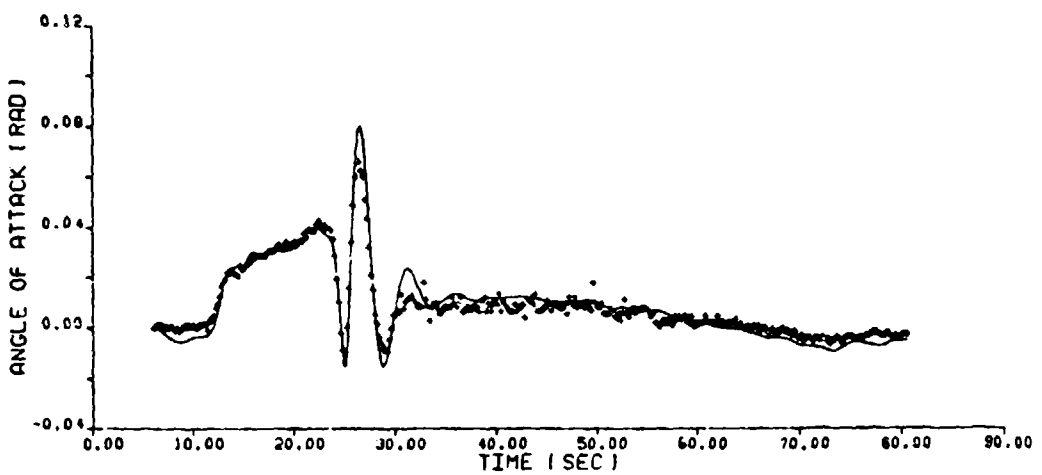

Phugoid Time History With Seven Parameters Estimated

Figure 9
APPENDIX D
Page 1 of 3

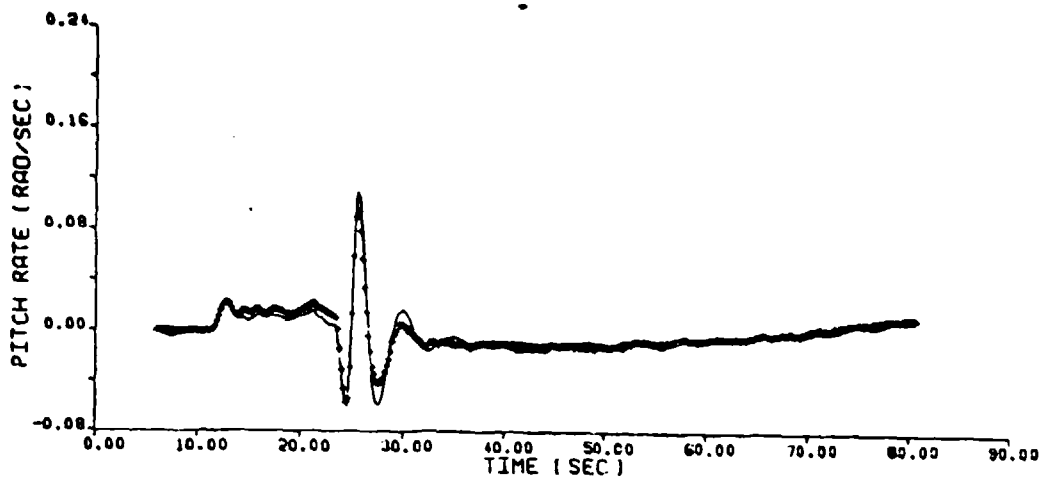

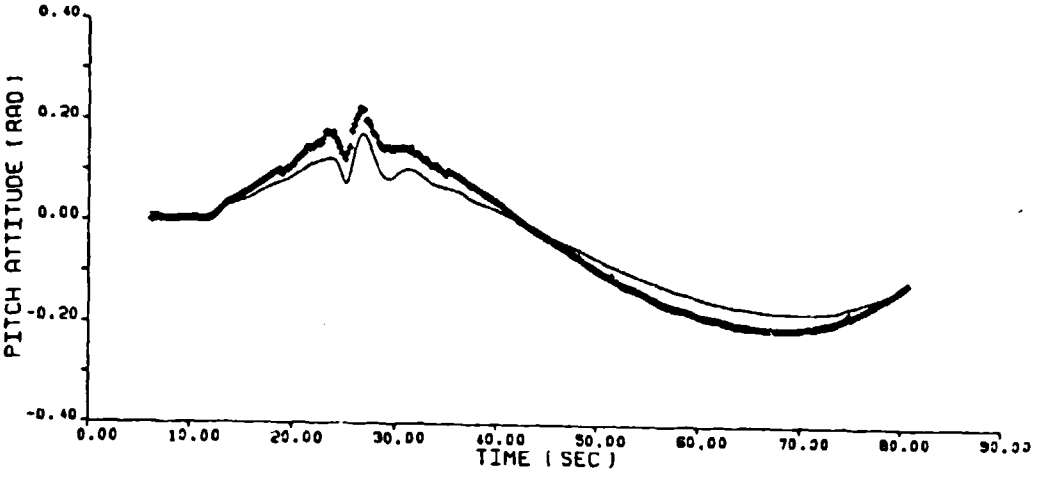

Phugoid Time History With Seven Parameters Estimated

Figure 9
APPENDIX D
Page 2 of 3

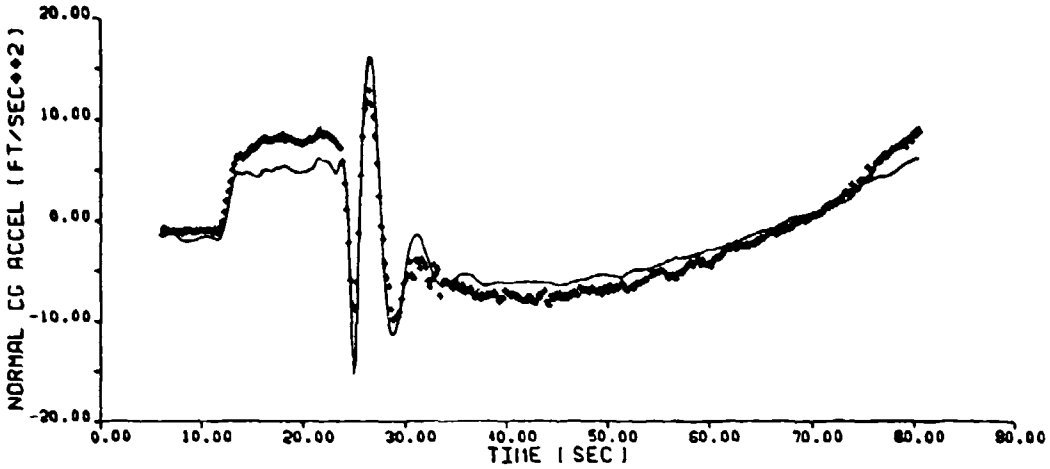

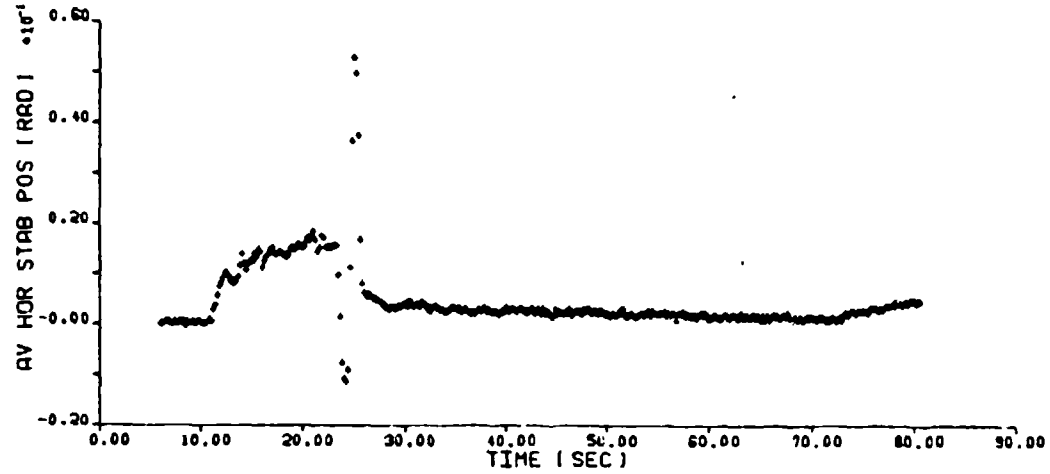

Phugoid Time History With Seven Parameters Estimated

Figure 9
APPENDIX D
Page 3 of 3

LIST OF REFERENCES

1. Naval Air Test Center contract N00014 - 72 - C - 0328, SCIDNT (SCI Maximum Likelihood Identification), 1971.

2. Benjamin, J. R. and Cornell, C. A., Probability, Statistics, and Decision for Civil Engineers, McGraw-Hill, 1970.

3. Systems Control, Inc., Technical Report No. 3, SCIDNT I, Theory and Application, by N. K. Gupta and W. E. Hall, December 1974.

4. Bryson, A. E., Jr. and Ho, Y. C., Applied Optimal Control, Blaisdell, 1969.

5. Naval Test Pilot School Flight Test Manual FTM-No. 103, Fixed Wing Stability and Control Theory and Flight Test Techniques, by Lcdr. S. D. Langdon, 1 August 1969.

6. Northrop Corporation Aircraft Division Report A2-61-4II, Dynamics Of The Airframe.

7. Grumman Aircraft Engineering Corporation Report A51-720-R-71-03, Demonstration Instrumentation Report F-14A #8 Bu. No. 157987 Code 26512, by J. Ryan, 21 June 1971.

8. Preliminary Natops Flight Manual Navy Model F-14A Aircraft, NAVAIR 01-F14AAA-1, 1 November 1973.

9. Grumman Aircraft Engineering Corporation Report A51-720-R-71-03, Demonstration Instrumentation Report F-14A #8 Bu. No. 157987 Code 26512, by J. Ryan, 1 October 1971.

10. XEROX Computer Systems Installation Bulletin 988108, Naval Air Test Center Real-Time Telemetry Processing System (RTPS), November 1973.

11. USAF Test Pilot School FTC-TIH-70-1001, Performance, January 1973.

INITIAL DISTRIBUTION LIST

		No. Copies
1.	Defense Documentation Center Cameron Station Alexandria, Virginia 22314	2
2.	Library, Code 0212 Naval Postgraduate School Monterey, California 93940	2
3.	Department Chairman, Code 57 Department of Aeronautics Naval Postgraduate School Monterey, California 93940	1
4.	Associate Professor R. A. Hess, Code 57He Department of Aeronautics Naval Postgraduate School Monterey, California 93940	1
5.	Mr. Roger Burton Special Projects Strike Test Directorate Naval Air Test Center NAS Patuxent River, Maryland 20670	5
6.	Naval Air Systems Command Attn: AIR-320D Washington, D.C. 20360	1
7.	Naval Air Systems Command Attn: AIR-5102 Washington, D.C. 20360	2
8.	Naval Air Systems Command Attn: AIR-5301 Washington, D.C. 20360	2
9.	Naval Air Systems Command Attn: 53014 Washington, D.C. 20360	2
10.	Naval Air Development Center Attn: AMFA-2 Warminster, Pennsylvania 18974	2
11.	Major Frederick T. Bryan, USMC 593A Michelson Road Monterey, California 93940	1

Manufacturing labor costs refer to all direct labor necessary to machine, fabricate, and assemble the major aircraft structure. This includes the direct labor portion of components that are built off-site. The labor necessary to install these components and purchased components is also included. Man-hours required to fabricate the purchased parts and materials are excluded (Ref 4:27-28).

Manufacturing materials include raw and semifabricated materials plus purchased parts and equipment used in the construction of the airframe. Purchased parts are general hardware items such as electrical fittings, valves, and hydraulic fixtures. Purchased equipment is other general purpose items such as actuators, motors, generators, landing gear, instruments, and hydraulic pumps. Such equipment may be purchased by the contractor or provided by the government. However, if a piece of equipment is specifically designed for a particular aircraft, it is considered subcontracted and excluded from manufacturing materials (Ref 4:31).